Quaternary Science Reviews 245 (2020) 106493

Contents lists available at ScienceDirect

Quaternary Science Reviews

journal homepage: www.elsevier.com/locate/quascirev

Holocene glacier change in the Silvretta Massif (Austrian Alps) constrained by a new ^{10}Be chronology, historical records and modern observations

Sandra M. Braumann [a, b, *], Joerg M. Schaefer [b], Stephanie M. Neuhuber [a], Jürgen M. Reitner [c], Christopher Lüthgens [a], Markus Fiebig [a]

[a] University of Natural Resources and Life Sciences (BOKU), Peter Jordan-Straße 82, A-1190, Vienna, Austria
[b] Lamont-Doherty Earth Observatory of Columbia University, Division of Geochemistry, Palisades, NY, 10964, USA
[c] Geological Survey of Austria, Neulinggasse 38, A-1030, Vienna, Austria

ARTICLE INFO

Article history:
Received 6 February 2020
Received in revised form
3 July 2020
Accepted 17 July 2020
Available online xxx

Keywords:
Holocene
Little Ice Age
Glacier change
Paleoclimate
Terrestrial cosmogenic nuclides
Surface exposure dating
Historical records
Austrian Alps
Silvretta Massif

ABSTRACT

Mountain glaciers are important water resources in Alpine regions and are sensitive to climate change. Reconstructing glacier oscillations improves our understanding of the amplitude and the frequency of climate variability and resolves time periods when the climate system was in transition – from glacial to interglacial conditions at the beginning of the Holocene, and from a naturally controlled system to an anthropogenically influenced system in the course of industrialization.

With this study, we contribute a new Holocene mountain glacier chronology from the Eastern European Alps. The study area, the Ochsental in the Silvretta Massif, features pronounced Holocene moraine ridges and is an important catchment for hydropower production. We present 18 new ^{10}Be exposure ages of bedrock outcrops (n = 2) and boulders (n = 16). We complement the ^{10}Be glacier chronology with historical records and instrumental time series and correlate it with pre-existing climate proxy records for capturing ice margin positions at different times during the Holocene. The Ochsental chronology is compared to cosmogenic nuclide moraine records across the European Alps to provide an Alpine-wide perspective on the transition from the Younger Dryas (YD; c. 12.9 to 11.7 ka) to the Holocene (c. 11.7 ka to present).

Results show that glaciers in the Ochsental stabilized at the position of a preserved Holocene moraine c. 9.9 ± 0.7 ka after retreating from their Late Glacial position. This Holocene moraine formation interval is concurrent with a cold spell detected in some climate proxy records in the Swiss and Austrian Alps, the Central European Cold Phase 1 (CE-1). Glaciers were presumably much smaller during the Mid-Holocene and readvanced to a position close to the preserved Early Holocene moraine during the Little Ice Age (LIA; c. 1250 to 1850 CE). LIA ^{10}Be ages range from 390 ± 20 yrs to 135 ± 5 yrs and point to multiple advances within this time period with most robust evidence for a culmination during the 18th century. The ^{10}Be record and the historical glacier records overlap and are remarkably consistent, which demonstrates that ^{10}Be surface exposure dating produces reliable ages even for young glacial deposits. Within the last c. 170 years, Ochsentaler glacier has retreated c. 2.3 km, which highlights the impact of recent warming on Alpine mountain glaciers.

1. Introduction

Alpine glaciers respond sensitively to climate change, from seasonal and annual to centennial and millennial time scales (e.g. Haeberli et al., 2007; Lüthi, 2014; Oerlemans, 2005). The vulnerability of Alpine glaciers to changing climate conditions is emphasized by substantial losses in length and mass throughout the past decades, triggered by the current warming trend. Atmospheric temperatures in the European Alps rose twice as much (c. +2 °C) from the 19th to the early 21st century relative to the mean temperature increase in the Northern Hemisphere during the same

* Corresponding author. University of Natural Resources and Life Sciences (BOKU), Peter Jordan-Straße 82, A-1190, Vienna, Austria
E-mail address: sandra.braumann@boku.ac.at (S.M. Braumann).

https://doi.org/10.1016/j.quascirev.2020.106493

time interval (Auer et al., 2007). Alpine environments are highly susceptible to climate change with glaciers having important functions for ecology, economy and society in these regions. Understanding mountain glaciers' long- and short-term responses to climate variability is relevant for society and the livelihood of Alpine communities. Glaciated catchments will experience severe changes within the upcoming decades. Shrinking and vanishing glaciers cause shifts in hydrological regimes and have effects on fresh water supply, energy production, biodiversity, agriculture and natural hazard mitigation measures (e.g. Brunner et al., 2019; Dirnböck et al., 2011; Farinotti et al., 2012; Gobiet et al., 2014; Kaser et al., 2010; Schaefli et al., 2019). Projections regarding the pace and magnitude of these changes are vital for preparing for these changes.

The last major and abrupt climate shift, which was purely driven by natural forcing, occurred c. 11.7 ka ago. During the Younger Dryas (YD; c. 12.9 to 11.7 ka; Alley, 2000; Rasmussen et al., 2006), the final cold lapse at the end of the Late Glacial, glaciers across the European Alps were far outboard their Holocene ice extents, which is evidenced by numerous dated Egesen moraines, the morphostratigraphical equivalent of the YD (e.g. Federici et al., 2008; Ivy-Ochs et al., 2006; Reitner et al., 2016). At the beginning of the Holocene (c. 11.7 ka), glaciers began to abandon their Late Glacial ice margin along with rising temperatures and retreated to higher elevations. Holocene climate is relatively stable compared to the YD, but frequent climate oscillations have caused glacier fluctuations within the past millennia, albeit at smaller amplitudes (e.g. Magny, 2004; Marcott et al., 2013; Mayewski et al., 2004; PAGES 2k Consortium, 2013; Wanner et al., 2008; Wanner et al., 2011). While during the Holocene Thermal Optimum (c. 10 to 5 ka), for instance, glaciers were smaller than modern glaciers (e.g. Goehring et al., 2011; Hormes et al., 2001; Ilyashuk et al., 2011; Ivy-Ochs et al., 2009; Nicolussi, 2010; Nicolussi et al., 2019; Nicolussi et al., 2005; Nicolussi and Patzelt, 2000; Solomina et al., 2015), a number of proxy records in the Alps indicate cooling around 5 ka, the onset of the Neoglacial, which caused glaciers to grow again (e.g. Deline and Orombelli, 2005; Magny et al., 2006; Patzelt, 1973; Simonneau et al., 2014). A prominent expression of this cold phase was the Little Ice Age (LIA) between c. 1250 and 1850 CE (e.g. Grove, 2004; Mann, 2002; Matthews and Briffa, 2005; Nicolussi et al., 2006). Temperatures during the LIA dropped below the average of the preceding millennia (Luterbacher et al., 2016; Mann et al., 2008; PAGES 2k Consortium, 2013) and caused glaciers to extend several hundred of meters beyond the modern ice margin (e.g. Ivy-Ochs et al., 2009; Solomina et al., 2015; Solomina et al., 2016). Although the LIA and corresponding glacier responses were heterogenous across time and space, prominent phases of glacier advance are documented during the 14th, 17th and 19th century in the Alps (e.g. Holzhauser et al., 2005; Ivy-Ochs et al., 2009; Nicolussi, 2013; Nicolussi and Patzelt, 2001; Nussbaumer and Zumbühl, 2012; Zumbühl and Nussbaumer, 2018). Since the beginning of industrialization, natural climate variability is increasingly superimposed by anthropogenic impact. Human activities have triggered another, man-made and ongoing climate transition, which has led to a synchronous and global retreat of most mountain glaciers over the past decades (e.g. Marzeion et al., 2014; Reichert et al., 2002; Vaughan et al., 2013).

A wealth of proxy records has improved our current understanding of Holocene glacier and climate change in the Alps. Radiocarbon records derived from the dating of various types of organic material (e.g. charcoal, peat, subfossil wood, human remains, etc.), which was found in (recently) deglaciated catchments, provide evidence of tree and peat growth, and human activities in high-mountainous regions (e.g. Bonani et al., 1994; Holzhauser et al., 2005; Nicolussi and Patzelt, 2001; Röthlisberger, 1976; Schneebeli, 1976). Dendrochronologies that in the European Alps reach back more than nine millennia allow assigning calendar dates to tree logs found in glacial deposits or along melting ice margins (e.g. Joerin et al., 2008; Le Roy et al., 2015; Nicolussi et al., 2009; Nicolussi and Schlüchter, 2012). Sedimentary, palynological and/or biotic analyses of speleothems, lake sediments and peat cores inform us on climatic and hydrological conditions in the past (e.g. Festi et al., 2016; Heiri et al., 2014; Ilyashuk et al., 2009; Luetscher et al., 2011).

Over the last 25 years, Surface Exposure Dating (SED) of moraines has enabled reconstructions of past glacier culminations with increasing precision and accuracy (e.g. Balco, 2011; Phillips et al., 2016; Rood et al., 2010). Some pioneering cosmogenic nuclide studies have addressed the YD and the Early Holocene (EH) time scale by dating moraines between Late Glacial and LIA moraines and have assigned numerical ages to relative moraine stratigraphies (Ivy-Ochs et al., 2007; Kerschner and Ivy-Ochs, 2008). However, an Alpine-wide correlation of theses moraines is complicated: First, there are fewer YD-EH cosmogenic nuclide moraine chronologies in the Eastern Alps than in the Central and Western Alps (Fig. 1). A large-scale perspective on the YD-EH transition is thus challenging. Second, there is age variability among YD-EH moraines preserved in different Alpine valleys (Ivy-Ochs, 2015). Uncertainties inherent to the SED method are manageable today, whereas geomorphological uncertainties are problematic to control and likely cause temporal variability among different moraine chronologies. Another explanation for age variability could be differences in moraine preservation between valleys, or inhomogeneity in glaciers' responses to EH warming.

Some proxy records in the Eastern Alps show that glaciers have already retreated to positions close to, or even inboard their LIA maxima around 10 ka (e.g. Koinig et al., 2019; Nicolussi, 2011; Nicolussi and Patzelt, 2000; Patzelt, 2016; Patzelt and Bortenschlager, 1973). In turn, a SED study at Kromer- and Klostertal – two valleys neighboring our study site – contradict these findings. In these valleys, lateral and frontal moraines were identified some hundreds of meters outboard the LIA maximum and were dated to c. 10 ka (Kerschner et al., 2006; Moran et al., 2016b). The controversy of several proxy records indicating significantly smaller glaciers relative to the Kromer type locality has led up to the question, if it is possible that glaciers respond differently to climate change even on a local scale, or if this discrepancy is due to geomorphological uncertainties.

The main objective of this paper is therefore to contribute a comprehensive Holocene moraine chronology from the Ochsental, a glaciated valley in the Silvretta Massif, and to temporally and spatially constrain Holocene ice margins. We aim to improve our understanding of glacier and climate systems in transition, and provide information on the natural baseline of climate variability prior to industrialization, upon which recent climate and glacier change has been forced. The moraine chronology includes the first LIA ^{10}Be exposure ages in the Eastern Alps and overlaps with historical and instrumental glacier data, which we use to evaluate the validity of the youngest ^{10}Be ages. We discuss our results within the framework of existing climate and glacier proxy records, the historical record (historical maps and documents) and the instrumental time scale (time series of temperature and glacier change), with the goal to compile an improved record of Holocene glacier dynamics in the Silvretta Massif. Specifically, we intend to test (1) whether the timing and magnitude of Holocene glacier advances in our study area are consistent with patterns reported by comparable studies conducted in the Central and Western Alps, (2) whether ^{10}Be SED is apt to resolve the fine structure of LIA glacier culminations, and (3) whether the youngest ^{10}Be ages are in agreement with ice margin positions inferred from historical documents and maps.

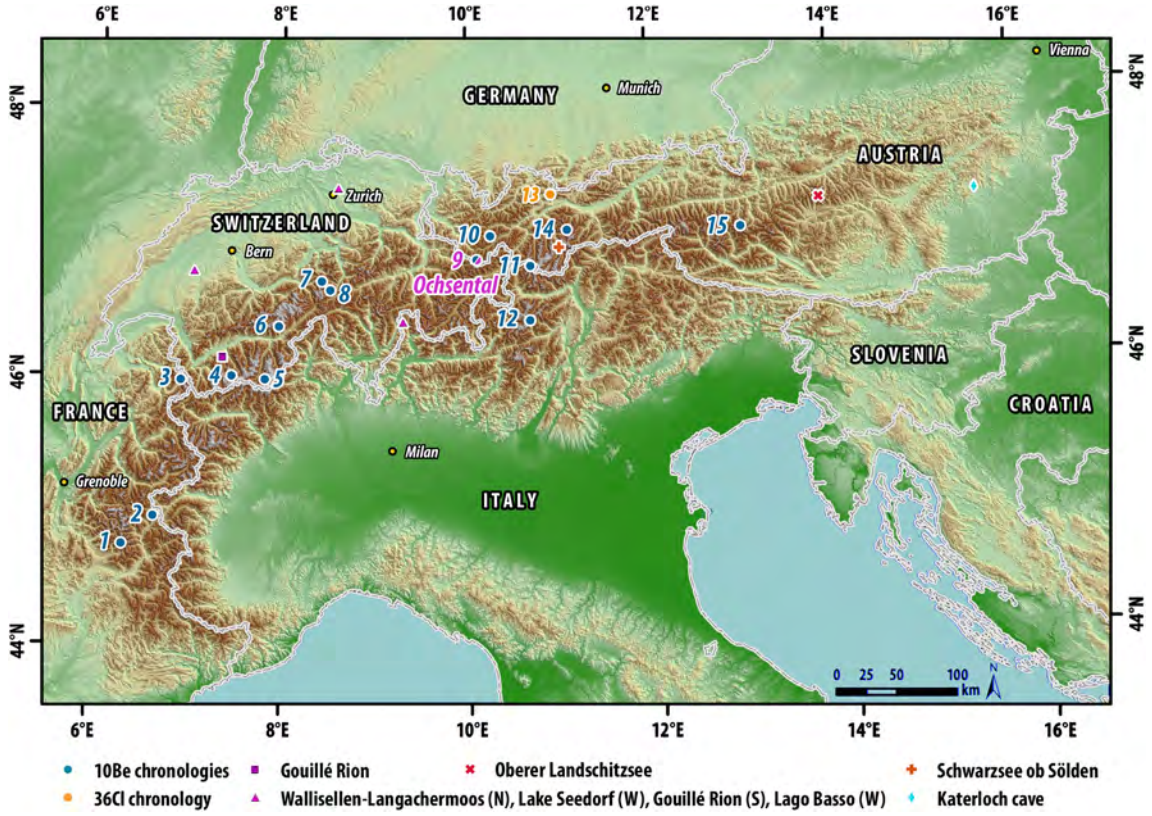

Fig. 1. Overview of the European Alps; the study area "Ochsental" in the Silvretta Massif is shown in pink. ^{10}Be chronologies (blue dots) and ^{36}Cl chronology (orange dot), which include moraines deposited during the Younger Dryas (YD)-Early Holocene (EH) transition and/or during the Holocene are numbered from West towards the East: 1. Écrins-Pelvoux Massif – Champoléon valley (Hofmann et al., 2019; Le Roy et al., 2017), 2. Clarée valley (Cossart et al., 2012), 3. Argentière glacier (Protin et al., 2019) 4. Tsidjiore Nouve (Schimmelpfennig et al., 2012), 5. Triftje- and Oberseegletscher (Kronig et al., 2018), 6. Belalp (Schindelwig et al., 2012), 7. Steingletscher (Schimmelpfennig et al., 2014), 8. Göschenental (Boxleitner et al., 2019a) and Meiental (Boxleitner et al., 2019b), 9. Ochsental (this publication) and Kromertal (Kerschner et al., 2006; Moran et al., 2016b), 10. Kartell (Ivy-Ochs et al., 2006), 11. Falgin cirque (Moran et al., 2016a), 12. Upper Peio valley (Baroni et al., 2017), 13. Schwärzkar (Moran et al., 2017a), 14. Lisenser Tal (Moran et al., 2017b), 15. Rauris (Bichler et al., 2016). Locations of several climate proxy records in the Central and Eastern Alps: Gouillé Rion (Haas et al., 1998; Tinner and Kaltenrieder, 2005), Swiss Plateau including Gouillé Rion site (Haas et al., 1998), Schwarzsee ob Sölden (Ilyashuk et al., 2011), Oberer Landschitzsee (Schmidt et al., 2006) and Katerloch cave (Boch et al., 2009). (For interpretation of the references to color in this figure legend, the reader is referred to the Web version of this article.)

2. Background and regional setting

Over the past two decades, SED using terrestrial cosmogenic nuclides (TCN) has become a powerful tool for reconstructing past glacier oscillations in the Alps (e.g. Darnault et al., 2012; Dielforder and Hetzel, 2014; Ivy-Ochs, 2015; Ivy-Ochs et al., 2009; Kelly et al., 2004; Kerschner and Ivy-Ochs, 2008; Le Roy et al., 2017; Moran et al., 2016a; Moran et al., 2017b; Schimmelpfennig et al., 2012; Schimmelpfennig et al., 2014; Schindelwig et al., 2012). The principle of SED is the quantification of in situ produced radionuclide concentrations in glacial deposits such as moraines to derive exposure ages (e.g. Balco, 2011; Gosse and Phillips, 2001; Lal, 1988). In the majority of studies, the content of the cosmogenic nuclide ^{10}Be was analyzed to generate exposure ages of glacial deposits. However, the application of other cosmogenic nuclides such as ^{14}C, ^{26}Al and ^{36}Cl is becoming increasingly popular for determining complex exposure and burial histories of rock surfaces (e.g. Goehring et al., 2011; Hippe et al., 2014; Moran et al., 2017a; Wirsig et al., 2016). ^{10}Be moraine chronologies are inherently discontinuous given that ice margins of older ages but smaller extents were removed by younger but more extensive advances. However, ^{10}Be moraine records in combination with geomorphological mapping provide temporal and spatial information on phases when glaciers were in advanced and stable positions. They are key for directly capturing glacier culminations and atmospheric changes in the past.

The Silvretta Massif in the Eastern Alps is an East-West oriented mountain chain located at the border of Austria and Switzerland. With an elevation of 3312 m a.s.l., Piz Buin is the highest peak in the region. The upper sections of catchments surrounding Piz Buin are glaciated. Ochsentaler and Vermunt glaciers with areas of c. 2.1 km^2 and c. 1.3 km^2 (in 2017), respectively, are located on the northern flank of the mountain range and are among the most extensive ice bodies left in the region (Fig. 2). Both glaciers are draining into the Ochsental and were converging during colder periods such as the LIA, when their termini have been in advanced positions. The mean annual atmospheric temperature between 1981 and 2010 CE observed at the meteorological station closest to our study site amounts to 3.1 °C (Galtür; station number 101949; 1587 m a.s.l.; BMNT, 2016). The mean annual precipitation rate over the same reference period was 1087 mm/yr and is generally highest in August.

Geologically, our study site is part of the Silvretta-Seckau nappe system, which forms the base of the Upper Austroalpine unit. The Silvretta nappe itself consists of metamorphic rock, with mainly variscan and subordinate alpidic deformation ages (Schuster, 2015). Lithology in the Ochsental is thus dominated by metamorphic rocks such as amphibolites and orthogneiss with low quartz contents ranging from c. 1–10% in our samples (Bertle, 1973; Fuchs and Oberhauser, 1990; Nowotny et al., 1993).

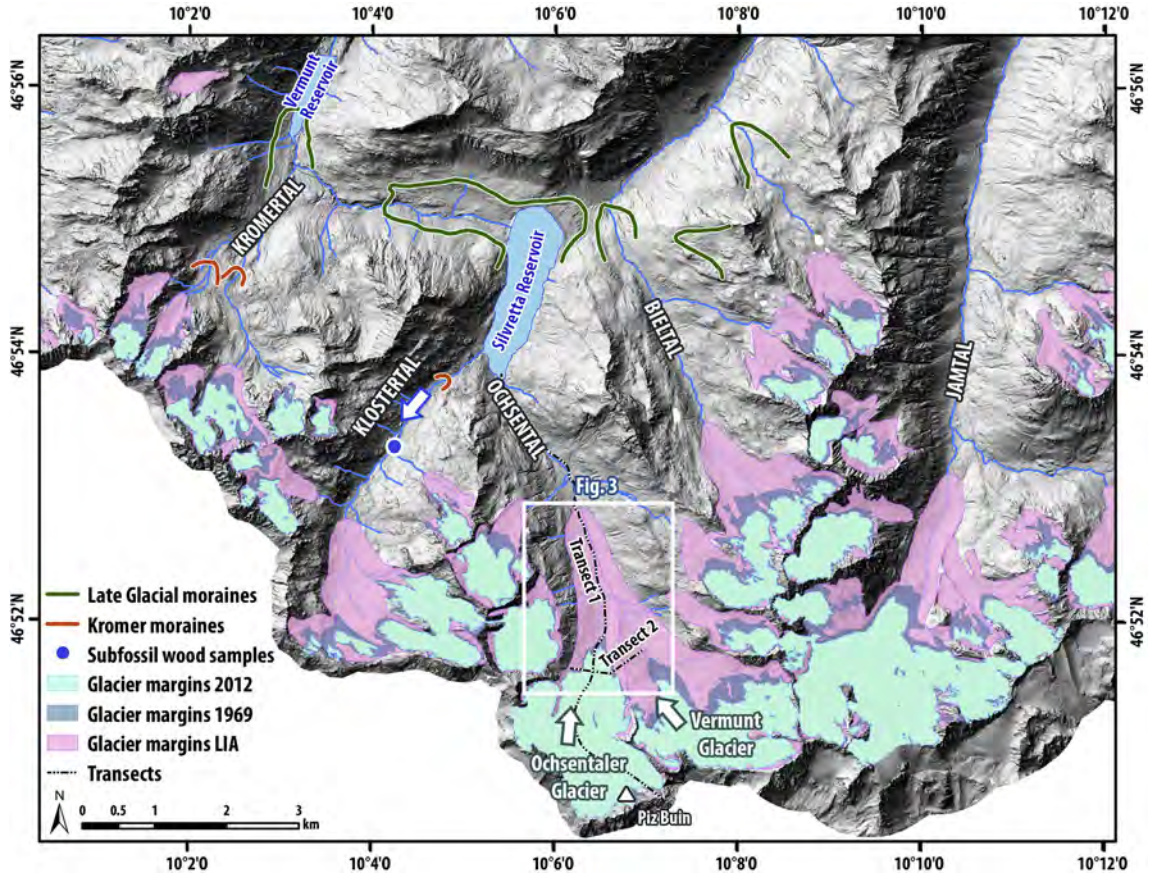

Fig. 2. Ice margin map of the north-facing central part of the Silvretta Massif with locations of pre-existing geomorphological and geochronological information. An (undated) ice margin (green) below the Silvretta reservoir is adopted from Hertl (2001), who assigned it to the "Egesen-III", equivalent of the final phase of the Younger Dryas (YD). Kromer moraines at Kromertal and Klostertal (orange lines) were mapped by Gross et al. (1978) and were dated with ^{10}Be Surface Exposure Dating (SED) by Kerschner et al. (2006) and Moran et al. (2016b). At Klostertal, subfossil wood was found in peat bogs at altitudes of 2125 m a.s.l. (in the vicinity of the Kromer moraine) up to an elevation of 2200 m a.s.l. (blue dot). Samples were dated using a combination of dendrochronological and radiocarbon dating (Gross, 2015; Nicolussi, 2010; Nicolussi et al., 2009). Ice margins from the Little Ice Age (LIA) and from the years 1969 and 2012 are inferred from the Austrian Glacier Inventory (AGI; Fischer et al., 2015, and references therein). New ^{10}Be boulder and moraine ages presented in this study are located in the upper valley section of Ochsental (white rectangle). Positions of transects shown in Fig. 9 are indicated by black dotted lines. Digital Elevation Models (DEMs) provided by © Land Vorarlberg – data.vorarlberg.gv.at (resolution 0.5 m), and © Land Tirol (resolution 1 m). (For interpretation of the references to color in this figure legend, the reader is referred to the Web version of this article.)

The Silvretta Massif ridge is a major drainage divide in Europe and is important with respect to the regional hydrological regime. While the north-facing side drains into the Rhine catchment and subsequently into the North Sea, the southern flank is part of the Danube catchment draining into the Black Sea. Runoff towards the north is used to generate electricity with multiple reservoirs and hydropower plants deployed downstream. Hydropower production in the northern Silvretta catchment and surrounding glaciated areas is important for the regional energy supply. In the year of 2017, hydropower plants in the region contributed 7.9% to Austria's hydropower production (3056 GWh in 2017), equivalent to 2.1% of Austria's total energy production (BMNT, 2018; Vorarlberger Illwerke AG, 2017). One of the largest reservoirs in the area, the Silvretta reservoir, is located at c. 2000 m a.s.l., at the entrance of Ochsental and adjacent Klostertal (Fig. 2). It stores precipitation and melt water discharged from both valleys. C. 6 km^2 of the catchment area are still glaciated, implying that melt water contributes significantly to today's hydropower production. Short-term, shrinking glaciers cause increased runoff due to melt water, adding to the total runoff. However, on a decadal time scale with continuously increasing summer temperatures, the water storage capacity of glaciers during winter seasons and water supply during summer seasons are expected to diminish (EEA, 2009). Current and near-future hydrological changes related to retreating Silvretta glaciers directly influences socio-economy and demand a detailed understanding of the regional climate system in general, and the rate of these changes in particular, to inform and optimize adaption strategies.

3. Geomorphological description

In the Ochsental, footprints of former glacier margins are found just below today's Silvretta reservoir, where Hertl (2001) mapped ice margins, whose age of deposition he placed into the Egesen-III phase (Fig. 2) corresponding to the final episode of glacier advance during the YD prior to a phase of rapid ice decay at the beginning of the Holocene (e.g. Cossart et al., 2012; Darnault et al., 2012; Hofmann et al., 2019; Ivy-Ochs et al., 2009; Ivy-Ochs et al., 2006; Schindelwig et al., 2012). Upstream, first unequivocal geomorphological evidence of a younger Holocene ice margin is found at an elevation of c. 2165 m a.s.l. in the Ochsental (① in Figs. 3 and 4a). The terminal moraine is c. 10–12 m wide, is on average c. 2.5 m high and exhibits two to three sub-ridges in frontal and lateral sections (Fig. 5a). It is clast-supported, dominated by boulders some of which have volumes of several cubic meters. Both lateral moraines have similar dimensions, but the abundance of fine matrix

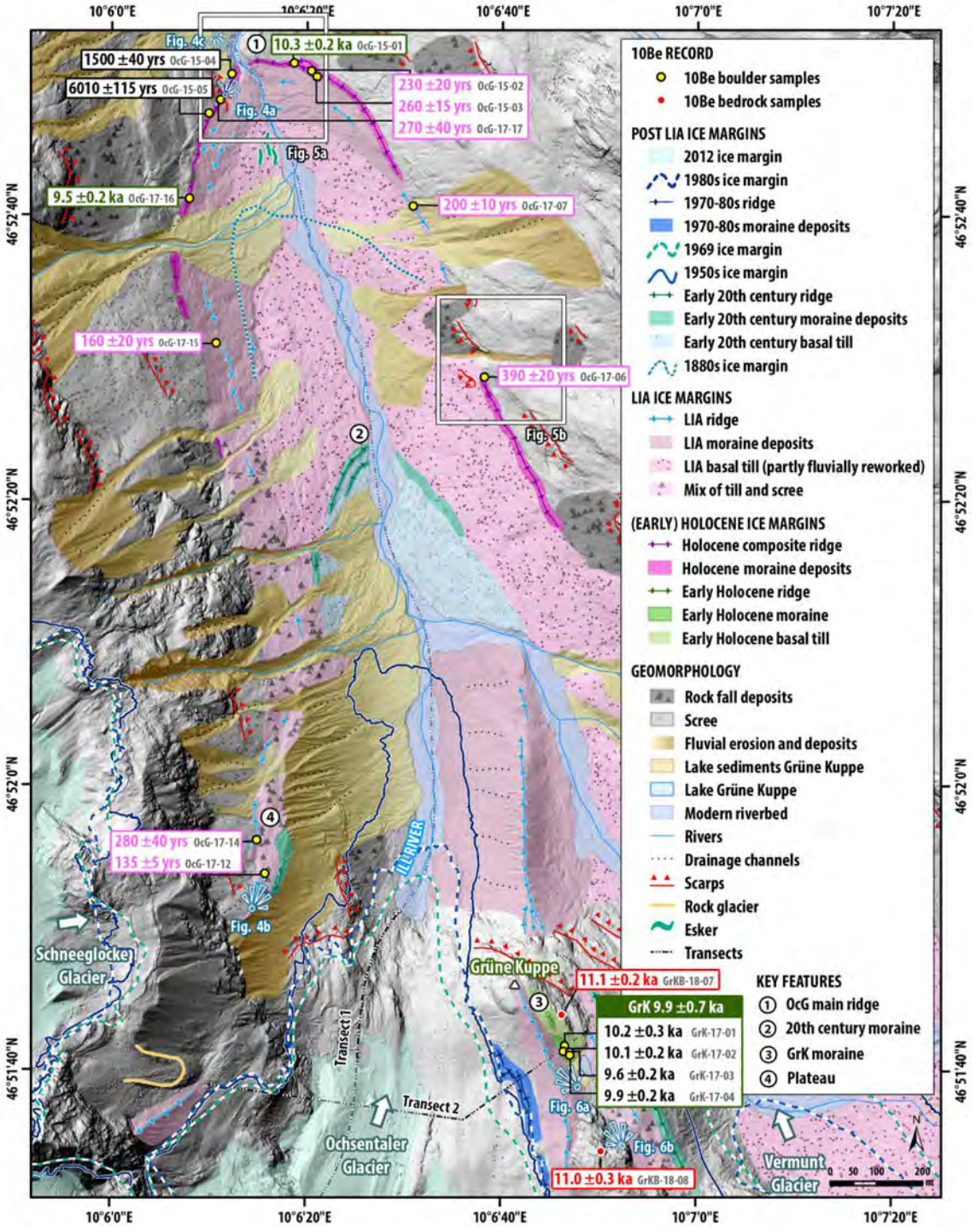

Fig. 3. Geomorphological map of Ochsental showing Holocene ice margin positions and ^{10}Be ages. Moraines were identified by ground-truth mapping and by evaluating Digital Elevation Models (DEMs). Early Holocene (EH) bedrock ages are colored in red, EH boulder ages are green, ages younger than the EH, but older than the Little Ice Age (LIA) are displayed in black and LIA ages are pink. Based on four consistent EH boulder ages, a landform age of 9.9 ± 0.7 ka was determined for the Grüne Kuppe (GrK) moraine (③). LIA ^{10}Be exposure ages are largely consistent with geomorphological conclusions in preceding mapping campaigns (Fischer et al., 2015, and references therein; Hertl, 2001; Vorndran, 1968) with the exception of Grüne Kuppe, which according to our ^{10}Be data was not covered with glacial ice during the LIA, hence suggesting an update of the Austrian Glacier Inventory (AGI) in this section. Early 20th century ice margins are inferred from historical maps and photographs. 1950s and 1980s ice margin positions are derived from aerial pictures. The 1969 and the 2012 ice margins are adopted from the AGI (Fischer et al., 2015). Positions of transects shown in Fig. 9 are indicated by black dotted lines. DEM provided by © Land Vorarlberg – data.vorarlberg.gv.at (resolution 0.5 m). (For interpretation of the references to color in this figure legend, the reader is referred to the Web version of this article.)

increases uphill. In these sections, the moraine is composed of matrix-supported diamict with fewer boulders deposited on the ridge. The left lateral moraine can be tracked up to an elevation of c. 2260 m a.s.l. into an area where hillslope gradients increase. It is likely that this terrain did not favor sediment accumulation due to its steepness. Any glacial deposits might have been transported subsequently downstream gravitationally and/or fluvially. Along its right lateral section, the moraine is largely preserved up to an

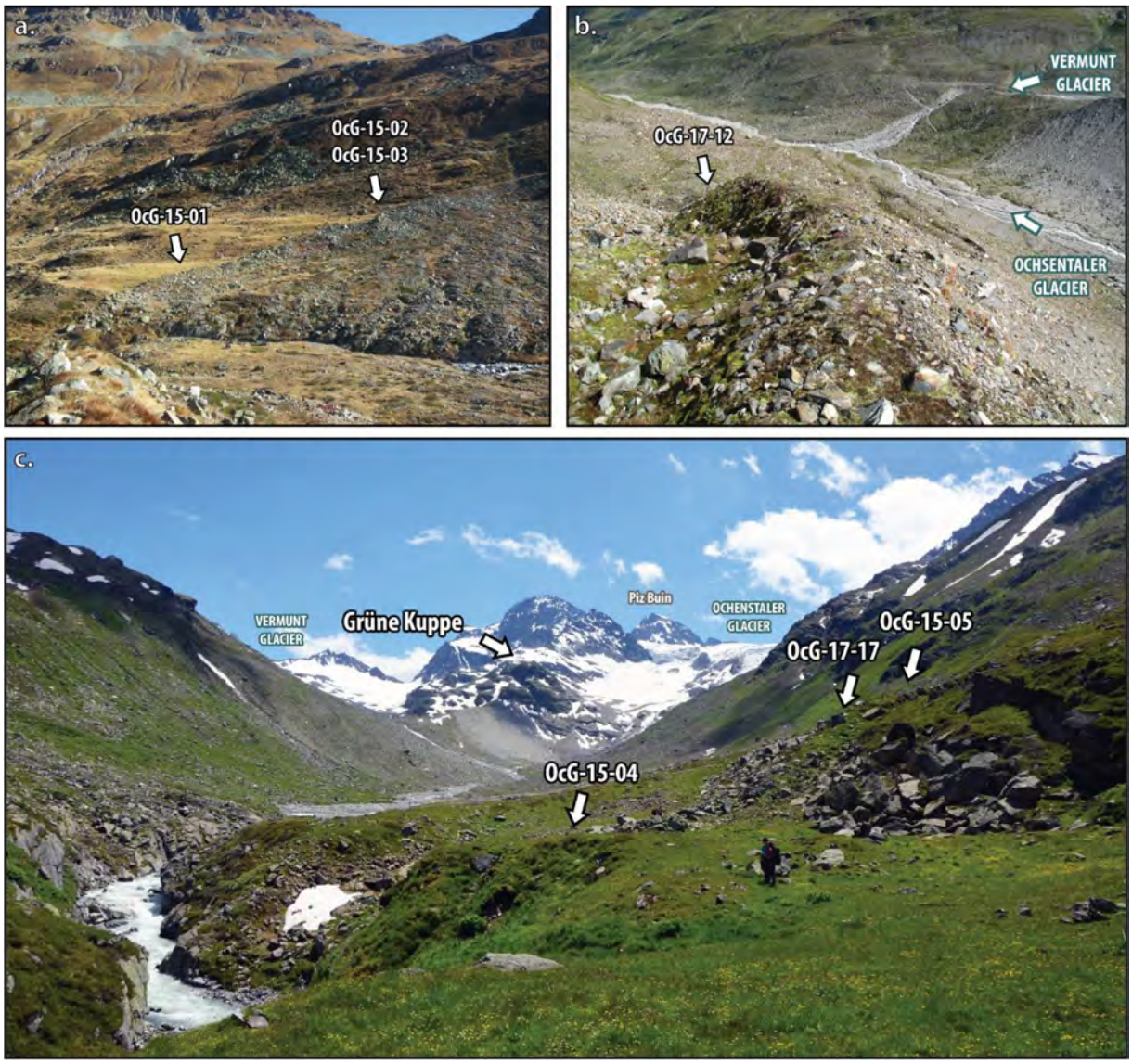

Fig. 4. Photographs of samples sites: **a.** Terminal moraine section ('OcG main ridge') in the Ochsental (① in Fig. 3). Boulder OcG-15-01 yields an age of 10.3 ± 0.2 ka, boulders OcG-15-02 and OcG-15-03 date to 230 ± 20 yrs and 260 ± 15 yrs. **b.** Left-lateral moraine set (④ in Fig. 3) in the Ochsental. Boulder OcG-17-12 with an age of 135 ± 5 yrs is embedded in the lower section of the moraine. To the right of the moraine in the center of the photo, there are two subsequent ridges, which mark ice margins during the early 20th century. **c.** Terminal moraine section (① in Fig. 3); Vermunt and Ochsentaler glaciers framing Grüne Kuppe in the background. Locations of ^{10}Be samples OcG-15-04 (1500 ± 40 yrs), OcG-15-05 (6010 ± 115 yrs) and OcG-17-17 (270 ± 40 yrs) along the main ridge are indicated with arrows. Note the discontinuity in riverbed geomorphology on the glacier-distal versus the glacier-proximal side of the terminal moraine. On the glacier-distal side of the OcG main ridge, the Ill river has eroded several meters into gneissic bedrock as opposed to the glacier-proximal side, where a braided river system has developed. On the right section of the photo, a bedrock outcrop is visible.

elevation of 2350 m a.s.l. Vegetation on the glacier-distal side of the ridge differs from the glacier-proximal side. While the valley floor towards the Silvretta reservoir is covered with a humus layer of several centimeters thickness and vegetated with characteristic Alpine flora, the glacier-proximal side of the moraine is dominated by pioneer plants growing on glacial till. River incision is distinct on either side of the moraine. On the moraine's glacier-distal side, the Ill river has carved a channel of several meters depth into the bedrock, whereas on the glacier-proximal upstream side the river is braided and does not show significant vertical erosion (Fig. 4c). In this area, to the left-lateral side of the braided Ill river, several eskers are preserved. These deposits consisting of rounded sand and gravel are remnants of subglacial meltwater channels, which developed beneath the glacier during the LIA and were exposed c. 150–170 years ago. The moraine, which we refer to as 'OcG main ridge' in the following, was mapped as LIA ice margin of Ochsentaler and Vermunt glaciers (Fischer et al., 2015, and references therein; Hertl, 2001; Vorndran, 1968). Nine ^{10}Be samples were taken from frontal and lateral sections of OcG main ridge boulders. We also sampled a boulder inside the LIA ice margin, which is plugged into the left lateral valley side (OcG-17-15).

At position ② in Fig. 3, at an elevation of c. 2210 m a.s.l., the next terminal moraine sequence is preserved and indicates a phase of glacier advance younger than LIA culminations. At its left lateral side, two blocky ridges have formed, which are mirrored towards the right of the Ill river in the form of linearly oriented boulders.

In the upper part of Ochsental, Grüne Kuppe (German for 'Green Crest'), a prominent elevated bedrock section partly covered with vegetated basal till is separating Ochsental (W) and Vermunt (E) glaciers (③ in Figs. 3 and 6). Grüne Kuppe is east- and westwards

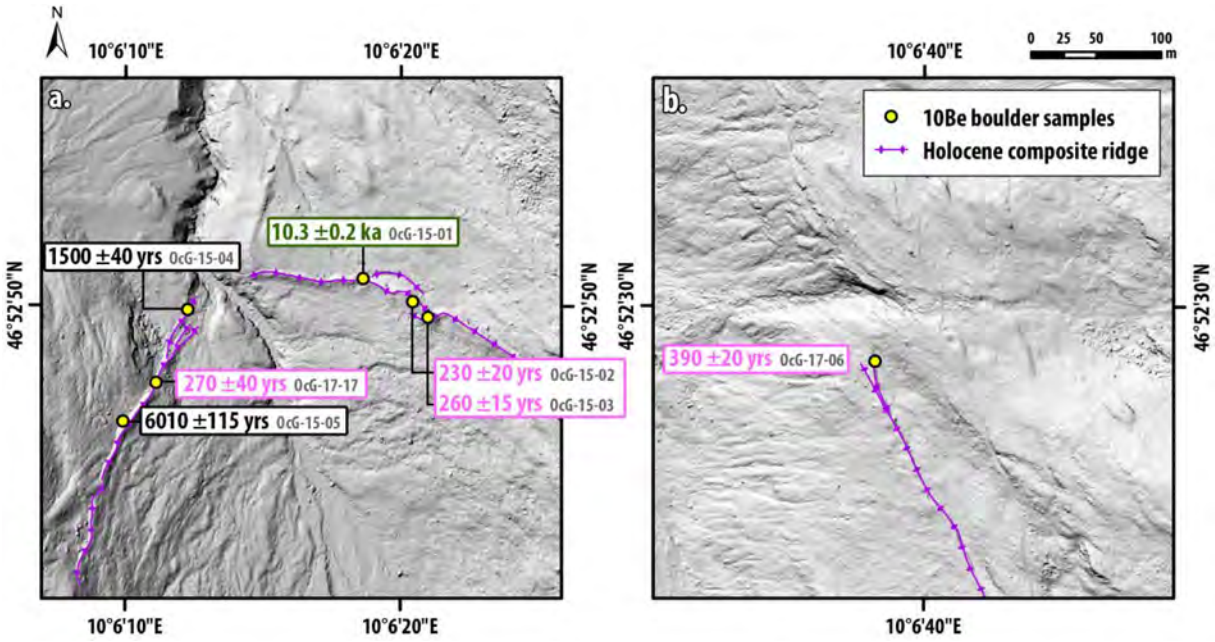

Fig. 5. Enlargement of selected ^{10}Be sample locations. **a.** Frontal section of the Ochsental moraine with multiple sub-ridges branching off the main ridge ①. **b.** Right lateral section of the Ochsental moraine, where a double-ridge structure was identified. One ^{10}Be rock sample was collected from the outer more prominent feature.

framed by moraine ridges consisting of barely weathered glacial debris. In between these young ice margin deposits, a smaller moraine ('GrK moraine') is identified (c. 6 m in width, c. 40 m in length and c. 2.5 m in height). The moraine is matrix-supported and features several boulders, which show weathered surfaces with considerable lichen populations, suggesting a longer period of exposure. Four boulders were sampled from this landform (GrK sample set). Additionally, we took two adjacent bedrock samples, one of them located at the northern edge of Grüne Kuppe (GrKB-18-07), and one at a position further uphill, on a higher elevated

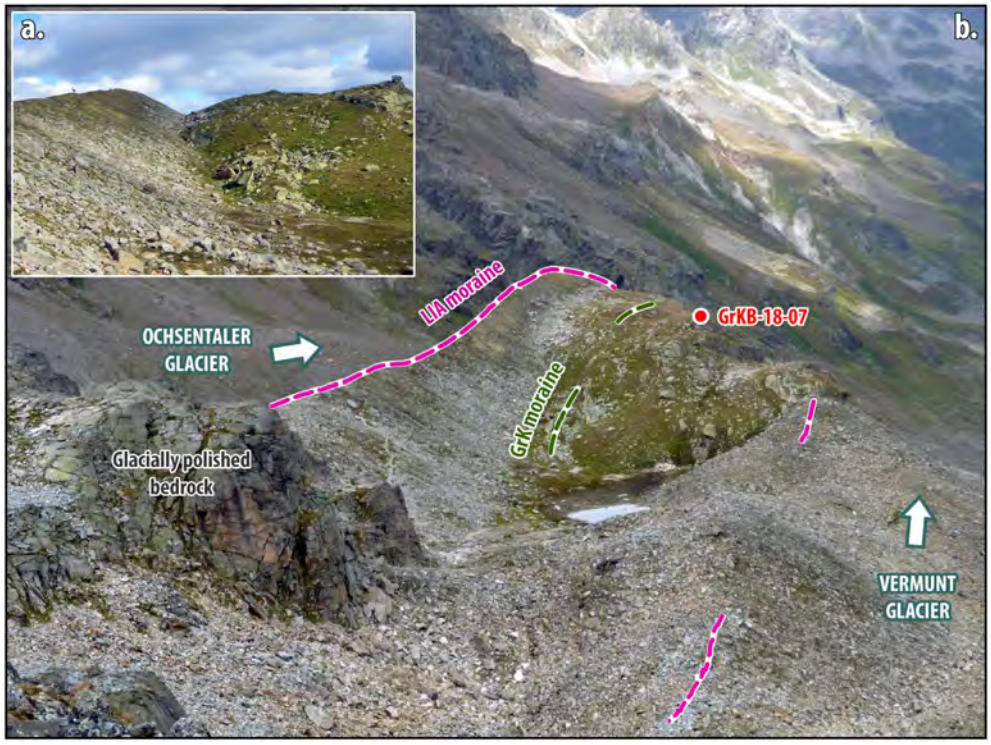

Fig. 6. Grüne Kuppe (③ in Fig. 3) **a.** Frontal view of Grüne Kuppe (GrK) moraine in the center and the Little Ice Age (LIA) moraine to the left. An ibex on top of the left moraine serves as scale. **b.** Grüne Kuppe, which translates to "Green Crest", was bracketed by former Ochsentaler (W) and Vermunt (E) glaciers. Note the difference in color of young LIA glacial debris (grey) and older glacial sediments of GrK moraine and its surroundings. Bedrock sample GrKB-18-07 was taken from the top of the bedrock outcrop (red), four boulder samples were taken along the Grüne Kuppe moraine.(For interpretation of the references to color in this figure legend, the reader is referred to the Web version of this article.)

level of bedrock outcrops (GrKB-18-08).

At the left lateral side of Ochsental, on a small plateau, a set of three moraines is identified (④ in Figs. 3 and 4b). The outer, glacier-distal ridge's main components are cobbles and boulders, whereas the inner two ridges are rich in fine sediments with fewer boulders on top. We sampled two boulders from the outer ridges on the plateau (OcG-17-12 and OcG-17-14).

4. Material and methods

4.1. Boulder and bedrock sampling for ^{10}Be surface exposure dating

Glacial landforms were first remotely mapped by evaluating Digital Elevation Models (DEMs) and aerial photos. Ground-truth geomorphological mapping and the collection of 18 ^{10}Be samples was carried out in the course of field campaigns in the years of 2015–2018. The sampling year is denoted by the first number in the sample ID; for instance, OcG-15-01 indicates sample collection in the year of 2015.

Criteria, which had to be met by boulders and bedrock sections in order to qualify for sampling are adopted from previous publications (e.g. Hebenstreit et al., 2011; Ivy-Ochs and Kober, 2008; Schaefer et al., 2006) and are also summarized in the appendix (S-Table 1). Sampling was accomplished with an electric saw and with hammer and chisel. Geographic locations of boulders were determined using a handheld GPS device with a lateral accuracy of 1–2 m. Sample elevation and topographic shielding were deduced from a DEM with a lateral and vertical resolution of 0.5 m. Orientation and dip of the sampled surface were measured using a geological compass. For a detailed documentation of boulders sampled for ^{10}Be analyses in the Ochsental, we refer to the appendix – section 4.

4.2. ^{10}Be sample processing and age calculation

Mechanical processing steps of all rock samples were accomplished at the Vienna Laboratory for Cosmogenic Nuclides. Whole rock samples were crushed using a jaw crusher targeting grain sizes between 75 and 355 μm. All chemical processing steps were carried out at the Lamont-Doherty Earth Observatory (LDEO) according to the protocol described in Schaefer et al. (2009). Quartz enrichment strategies included magnetic separation, froth flotation, multiple leaches using a mix of 5% HF and 5% HNO_3, and ultrasonic leaches with mixes of 2% HF and 2% HNO_3. After isolation and purification of quartz, a split of each sample was analyzed using ICP-OES in order to test for the presence of native ^{9}Be. In all samples, ^{9}Be concentrations were at the range of blanks implying that none of the samples contained native ^{9}Be. Pure quartz samples were spiked with custom-made LDEO carriers made from deep-mine Beryl and were then dissolved in concentrated HF. Beryllium was separated following standard procedures including repeated evaporations with hydrochloric acid, sulfuric acid and ion exchange columns. Beryllium oxide was then mixed with niobium and loaded into stainless steel cathodes. The 18 samples were processed in four batches, each of them including one to two procedural blanks. Measurements of ^{10}Be/^{9}Be sample ratios were performed at the Center for Accelerator Mass Spectrometry (CAMS) at the Lawrence Livermore National Laboratory (LLNL). Samples were measured against the 07KNSTD3110 standard with a nuclide ratio of 2.85×10^{-12}.

^{10}Be concentrations are reported corrected for blanks and for boron, and with 1σ analytical uncertainties and uncertainties related to the carrier concentration (1%). The ^{10}Be background in procedural blanks was subtracted from the total number of ^{10}Be atoms in each sample and ranges from 0.02% to 8.90% depending on the total amount of ^{10}Be atoms measured (appendix – section 2). ^{10}Be ages are calculated using the online calculator formerly known as the CRONUS-Earth online calculator (v3), and applying the Swiss ^{10}Be production rate calibrated at the Chironico landslide (Claude et al., 2014). This production rate is in good agreement with various recent production rate experiments (Balco et al., 2009; Borchers et al., 2016; Fenton et al., 2011; Kaplan et al., 2011; Kelly et al., 2015; Martin et al., 2015; Putnam et al., 2012, 2019; Young et al., 2013) and has been used in previous studies in the Alps (e.g. Le Roy et al., 2017; Protin et al., 2019). In order to show the sensitivity of ^{10}Be ages to the application of different production rates, we recalculated ages by applying the northeastern North America (NENA) production rate (Balco et al., 2009) and the CRONUS default production rate (Borchers et al., 2016). For scaling production rates to Ochsental's geographic location, the time-dependent 'Lm' scheme was used (Lal, 1991; Stone, 2000). We did not apply any correction for snow cover as we sampled top sections of boulders and selected windswept locations, if possible. Also, snow thickness and duration are not well constrained for the Holocene time scale, which complicates a systematic correction for snow cover (e.g. Schimmelpfennig et al., 2014). Neither did we correct for erosion as we avoided the sampling of surfaces, which showed signs of significant weathering. The erosion rate often used in comparable studies (1 mm/ka; André, 2002) would shift our ages only marginally (c. 1%) and does not change our age interpretation.

Reported landform ages are the arithmetic means of individual boulder ages on that landform. Uncertainties of landform ages include the 1σ standard deviation associated with analytical uncertainties, carrier uncertainties (1%), and the production rate uncertainty (c. 6.3%), which was propagated in quadrature. Potential outliers were identified following the χ^2-test implemented in the online calculator.

4.3. Glacier change reconstructions based on historical and instrumental data

Glacier fluctuations in the Ochsental since the end of the LIA c. 1850 CE were reconstructed by evaluating historical maps and complementary historical documents such as paintings and old photographs (e.g. Gross, 2015; Rutzinger et al., 2013, and references therein). A pioneering and comprehensive mapping campaign, which aimed to outline ice margins based on field observations, was the 'Franzisco-Josephinische Landesaufnahme' mandated by the House of Habsburg and carried out between 1871 and 1887 CE (K. u. k. Militärgeographisches Institut, 1887, Blatt 5244). Updates were realized between 1908 and 1915 CE (K. u. k. Militärgeographisches Institut, 1908–1915, Blatt 5244) and 1934–1937 CE (K. u. k. Militärgeographisches Institut, 1934–1937, Blatt 5244) for the region. However, in these updates, it seems as if ice margin positions were adopted from the 1880s map, which contradicts records on glacier front variation in the study area (WGMS, 2018). Therefore, the historical maps from 1908 to 1914 CE and 1934–1937 CE are discarded from any further consideration. In general, the quality of the historical maps varies as ice margins are approximations of glacier configurations in the past. Therefore, our premise for including historical maps in our reconstruction is the availability of two independent sources from similar periods, which show consistent glacier configurations. This condition is met by the map published in the 1880s (K. u. k. Militärgeographisches Institut, 1887) and a panorama sketch of Ochsental from the year of 1888 (Immler and von Siegl, 1888).

Modern glacier change is addressed by evaluating photographs from the 20th century and aerial pictures, which have been produced since the 1950s (Kasper, 2013; Landesamt für Vermessung und Geoinformation, 2019). Ice margin reconstructions for the

years of 1969 and 2012 are based on lidar data and orthophotos (Austrian Glacier Inventory – AGI; Fischer et al., 2015). Records describing front variation from 1850 (Ochsentaler glacier) and 1902 (Vermunt glacier) to 2016 and mass balances in the years from 1991 to 1999 are provided by the World Glacier Monitoring Service (WGMS, 2018). A homogenized summer temperature series from the nearest meteorological station (Galtür) from 1896 to 2008 is adopted from the HISTALP project (Auer et al., 2007) and is complemented with recent atmospheric summer temperature data from 2009 to 2016 (BMNT, 2019).

5. Results

5.1. Geological glacier record – ^{10}Be surface exposure ages

^{10}Be analytical results and exposure ages are listed in Table 1 and are put into a spatial context in Fig. 3. The ^{10}Be record is presented in order of decreasing age, from the EH to the youngest historical ages. Bedrock ages are introduced first, followed by the presentation of boulder and landform ages. Inferred outliers will be addressed at the end of this section.

At Grüne Kuppe (③), samples from the two bedrock sites yield EH ages. GrKB-18-07 located at Grüne Kuppe's northern tip dates to 11.1 ± 0.2 ka. GrKB-18-08 collected from a bedrock outcrop located 40 m higher relative to the elevation of GrKB-18-07 gives a ^{10}Be age of 11.0 ± 0.3 ka. Together, these bedrock ages imply deglaciation of Grüne Kuppe around 11 ka ago.

Boulder ages in the Ochsental fall within two time intervals: the EH around 10 ka and the historical time period. Boulder ages from the Grüne Kuppe moraine (GrK-17-01, GrK-17-02, GrK-17-03 and GrK-17-04) range from 9.6 ± 0.2 ka to 10.2 ± 0.3 ka with an arithmetic mean of 9.9 ± 0.7 ka. The Grüne Kuppe landform age indicates moraine formation during the EH after Grüne Kuppe became ice-free. Two samples from the OcG main ridge (①) also date to the EH period. OcG-15-01 was deposited on the glacier-distal side of the ridge and gives an age of 10.3 ± 0.2 ka (Fig. 5a). OcG-17-16 sits on the crest and dates to 9.5 ± 0.2 ka. Although we cannot exclude that these boulders were pre-exposed, we note that the ages are consistent with the Grüne Kuppe landform age.

Historical ^{10}Be ages agree with assumptions from earlier mapping campaigns, which state that moraines featuring these ages were deposited during the LIA (Fischer et al., 2015; Hertl, 2001; Vorndran, 1968). Ages range from 390 ± 20 yrs (OcG-17-06) to 135 ± 5 yrs (OcG-17-12) and are in stratigraphic order (Fig. 7). The oldest historical age (OcG-17-06 with 390 ± 20 yrs) stems from a boulder on the glacier-distal side of the right-lateral part of OcG main ridge, in a section, where a small sub-ridge splits off (Fig. 5b). Based on the boulder age, we speculate that the outer ridge is an expression of a mid-LIA advance, while the inner feature has accumulated later during the LIA. A group of four historical ages clusters in the 18th century (OcG-15-02: 230 ± 20 yrs, OcG-15-03: 260 ± 15 yrs, OcG-17-14: 280 ± 40 yrs and OcG-17-17: 270 ± 40). The mean age calculated from these four boulders amounts to 260 ± 30 yrs. A slightly younger sample, OcG-17-07, is located along the right lateral side of Ochsental and gives a boulder age of 200 ± 10 yrs. Boulder OcG-17-15 was deposited at the left lateral valley flank inside the OcG main ridge and dates to 160 ± 20 yrs. The youngest ^{10}Be age of the Ochsental record, 135 ± 5 yrs, is assigned to sample OcG-17-12 in the plateau section (④). The boulder is embedded in a moraine, which is bracketed by an outer moraine featuring a boulder age of 280 ± 40 yrs (OcG-17-14), and an inner moraine, which was deposited during the early 20th century.

14 out of 16 boulder samples in the Ochsental date either to the EH, or to the LIA period. Two exceptions are OcG-15-04 (1500 ± 40 yrs) and OcG-15-05 (6010 ± 115 yrs). Both boulders might have experienced pre-exposure, which causes an overestimation of ages. In the case of OcG-15-05, an inherited nuclide inventory appears to be likely as the age falls within the Holocene Thermal Optimum, when glaciers were most likely smaller than today in the European Alps (e.g. Goehring et al., 2011; Hormes et al., 2001; Joerin et al., 2008; Nicolussi and Patzelt, 2000, 2001). Therefore, we reject OcG-15-05 from our moraine chronology. OcG-15-04 yields a Neoglacial age. Around 5 ka, climate in the European Alps began to change towards cooler and wetter conditions (e.g. Magny et al., 2006; Marcott et al., 2013; Simonneau et al., 2014) evidenced by glaciers readvancing from their Mid-Holocene minima (e.g. Badino et al., 2018; Deline and Orombelli, 2005; Holzhauser et al., 2005; Ivy-Ochs et al., 2009; Le Roy et al., 2017; Moran et al., 2017b; Schimmelpfennig et al., 2012; Solomina et al., 2015). The age of 1500 ± 40 yrs, although isolated, is plausible as it falls within a time period, when glaciers across the Alps were growing again.

For testing the sensitivity of ages to different production rates, we compared results using the Swiss production rate (Claude et al., 2014), the NENA production rate (Balco et al., 2009) and the default production rate used in the online calculator formerly known as the CRONUS-Earth online calculator (Borchers et al., 2016). Ages calculated with the Swiss and NENA production rate are in good agreement with a maximum deviation of 0.17%. Ages using the global production rate are c. 2.50–4.35% younger than the ages calculated with the Swiss production rate (appendix – section 3).

5.2. Historical glacier record – historical maps, photographs and temperature time series

The 1880s glacier extents illustrated in Fig. 8a and Fig. 8b are based on a map published in 1887 (K. u. k. Militärgeographisches Institut, 1887, Blatt 5244), when the ice margin of Vermunt and Ochsentaler glaciers was c. 350–380 m inboard the LIA terminal moraine at an elevation of c. 2175 m a.s.l. (Fig. 9a). This position agrees with a drawing from c. 1888 (Immler and von Siegl, 1888), which indicates that the head of Ill river was located at an elevation of c. 2172 m a.s.l. (Fig. 8c). During the early 20th century, both glaciers continued to retreat and split into two individual glaciers. Around 450 m further upstream relative to the 1880s position, Ochsentaler glacier deposited a subsequent moraine (Fig. 9a). The moraine build-up interval is constrained by front variation measurements of Ochsentaler glacier, which suggest a halt in the early 20th century (Fig. 10b). In addition, a photograph taken around 1931 shows configurations of Ochsental and Vermunt glaciers with the early 20th century moraine visible in the left lateral forefield, confirming that Ochsentaler glacier had abandoned the moraine by then (appendix – section 6). The formation of this moraine is probably related to low global land surface temperatures in the early 20th century (IPCC, 2014), possibly to a phase of cooler summer and autumn temperatures around 1920 in the Alps (Böhm et al., 2001), which lead to a standstill of many Alpine glaciers (e.g. Haeberli et al., 2007; Nussbaumer and Zumbühl, 2012).

5.3. Instrumental glacier record – orthophotos, lidar data and glacier inventories

In the time period between the 1930s and 1950s, the front of Ochsentaler glacier retreated c. 450–480 m to an elevation of c. 2260 m a.s.l. in the 1950s (Figs. 3 and 9a). Similar retreat upvalley occurred between 1950 and 1969. In the late 1970s and early 1980s, Ochsentaler glacier readvanced (Figs. 9a and 10b), synchronously with other glaciers in the Austrian Alps such as Gepatsch Ferner, Goldberg Kees and Vernagtferner (WGMS, 2018). This readvance is

Table 1
^{10}Be analytical data and resulting ages. Samples were measured at the Center for Accelerator Mass Spectrometry (CAMS) at Lawrence Livermore National Laboratory (LLNL). All samples were measured against the 07KNSTD3110 standard with a ratio of 2.85×10^{-12} and are corrected for boron. One to two procedural blanks were processed along with each batch of samples, whose ratios range from 5.4×10^{-16} to 7.8×10^{-17}. The total numbers of ^{10}Be atoms represent values prior to blank correction; ^{10}Be atom concentrations are corrected for the measured numbers of atoms in the procedural blanks. For details regarding the level of ^{10}Be in blanks relative to the samples, we refer to the appendix – section 2. Ages were calculated using the online calculator formerly known as the CRONUS-Earth online calculator (v3) and using the 'Lm' scaling scheme and the Swiss ^{10}Be production rate reported by Claude et al. (2014). Ages are calculated relative to the sampling year and are rounded to the nearest 5 years. Uncertainties associated with individual samples are given including the 1σ analytical error and the uncertainty on the carrier concentration (1%). The outlier (OcG-15-05) is denoted in italics.

Sample ID	Latitude [DD]	Longitude [DD]	Elevation [m a.s.l.]	Av. thickness [cm]	Shielding factor	Quartz weight [g]	^{9}Be carrier [g]	^{10}Be/^{9}Be ratio ±1σ analytical unc. (10^{-14})	Total ^{10}Be atoms ±1σ analytical unc. [atoms]	^{10}Be conc. ±1σ analytical unc. [atoms/g qtz]	^{10}Be exposure age ±1σ analytical and carrier unc. [yrs]	Sampling year
GRÜNE KUPPE ③BEDROCK												
GrKB-18-07	46.8616	10.1126	2578	1.1	0.9913	6.7465	0.1806	17.59 ± 0.33 (1.9%)	2186384 ± 40823	323421 ± 6039	11095 ± 210	2018
GrKB-18-08	46.8590	10.1137	2617	1.1	0.9913	13.0866	0.1812	34.47 ± 0.82 (2.4%)	4295601 ± 101709	327906 ± 7764	10990 ± 260	2018
GRÜNE KUPPE ③BOULDERS												
GrK-17-01	46.8610	10.1127	2561	1.5	0.9830	30.1448	0.1814	60.05 ± 1.51 (2.5%)	7532161 ± 189905	287196 ± 7241	10175 ± 255	2017
GrK-17-02	46.8609	10.1126	2560	1.0	0.9833	29.9631	0.1817	32.63 ± 0.62 (1.9%)	4100216 ± 77386	285109 ± 5381	10070 ± 190	2017
GrK-17-03	46.8609	10.1128	2559	0.9	0.9840	29.6024	0.1799	29.71 ± 0.56 (1.9%)	3696197 ± 69051	269786 ± 5040	9575 ± 180	2017
GrK-17-04	46.8609	10.1128	2556	1.3	0.9815	29.4213	0.1811	18.14 ± 0.36 (2.0%)	2272029 ± 44577	279193 ± 5478	9945 ± 195	2017
OcG MAIN RIDGE ① and ④												
OcG-15-01	46.8802	10.1049	2182	2.8	0.9629	18.7294	0.1819	32.26 ± 0.60 (1.9%)	4104640 ± 76291	219102 ± 4072	10315 ± 190	2015
OcG-17-16	46.8775	10.1020	2236	1.0	0.9613	25.5701	0.1784	26.60 ± 0.43 (1.6%)	3281874 ± 53603	210132 ± 3432	9475 ± 155	2017
OcG-15-05	*46.8792*	*10.1025*	*2193*	*1.2*	*0.9593*	*12.7801*	*0.1824*	*13.17 ± 0.25 (1.9%)*	*1679721 ± 32209*	*131355 ± 2519*	*6010 ± 115*	*2015*
OcG-15-04	46.8800	10.1032	2167	1.2	0.9621	13.9728	0.1825	3.62 ± 0.10 (2.8%)	462023 ± 13011	32995 ± 929	1500 ± 40	2015
OcG-17-06	46.8741	10.1104	2328	1.0	0.9605	29.0626	0.1787	1.37 ± 0.08 (5.7%)	169351 ± 9659	9802 ± 559	390 ± 20	2017
OcG-17-14	46.8650	10.1039	2480	1.8	0.9405	26.1078	0.1796	0.56 ± 0.08 (14.4%)	70138 ± 10089	7586 ± 1091	280 ± 40	2017
OcG-17-17	46.8795	10.1028	2184	1.1	0.9635	25.3906	0.1795	0.48 ± 0.07 (14.3%)	59024 ± 8439	6127 ± 876	270 ± 40	2017
OcG-15-03	46.8799	10.1056	2195	1.2	0.9624	19.2613	0.1822	0.91 ± 0.06 (6.2%)	116594 ± 7173	6002 ± 369	260 ± 15	2015
OcG-15-02	46.8800	10.1054	2191	2.6	0.9625	20.4775	0.1818	0.85 ± 0.08 (9.5%)	107694 ± 10276	5210 ± 497	230 ± 20	2015
OcG-17-07	46.8774	10.1083	2270	1.4	0.9570	28.8815	0.1811	1.65 ± 0.07 (4.3%)	206855 ± 8841	4832 ± 207	200 ± 10	2017
OcG-17-15	46.8747	10.1027	2251	0.8	0.9185	25.9286	0.1792	0.39 ± 0.05 (13.9%)	48479 ± 6754	3660 ± 510	160 ± 20	2017
OcG-17-12	46.8644	10.1042	2488	1.6	0.9455	26.4684	0.1787	0.94 ± 0.05 (5.6%)	116646 ± 6484	3639 ± 202	135 ± 5	2017

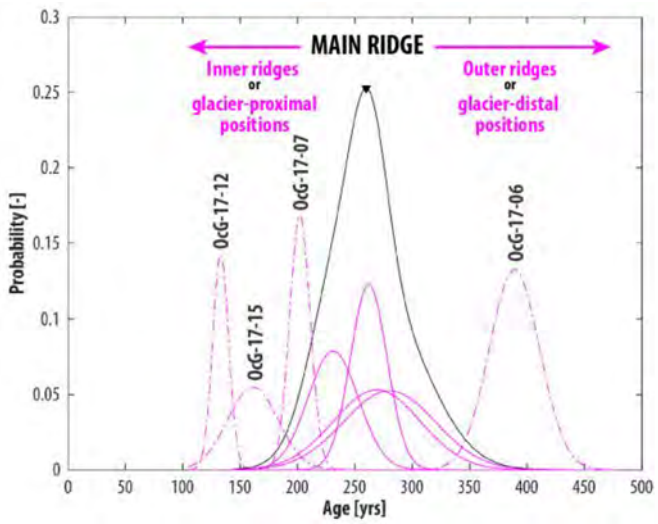

Fig. 7. Probability density function of boulder ages falling within the Little Ice Age (LIA) period. The plot highlights the stratigraphic order of ^{10}Be ages relative to the OcG main ridge.

probably caused by a drop of summer temperatures, which is observed in the study area (Fig. 10c) and which is consistent with the global temperature record (Blunden and Arndt, 2019; IPCC, 2014). Vermunt glacier has not responded to this climate signal and continued to retreat during this time period (Fig. 10b). Since the beginning of the 1990s, Ochsentaler and Vermunt glaciers have both been retreating with an accelerating rate in the order of tens of meters per year. Mass balances records are available for the years of 1991–1999 and are described using water equivalents (w.e.), the product of the snow height and the vertically-integrated snow density (Fig. 10a). Vermunt glacier shows a negative mass balance in all nine years with a maximum value of c. 1544 mm w.e. in 1998 and a minimum of c. 240 mm w.e. in 1995. Ochsentaler glacier has negative mass balances in seven of nine years, with 1120 mm w.e. in 1992 being the highest negative value. Positive mass balance values were detected in the years of 1995 and 1997 (maximum c. 50 mm w.e. in 1995). Total retreat of Ochsental and Vermunt glaciers over the last decade (2008/09 to 2018/19) amounts to c. 190 m and c. 170 m, respectively (Österreichischer Alpenverein, 2019).

6. Discussion

6.1. Younger Dryas-Early Holocene transition

Proxy records suggest that mean July temperatures were gradually rising in the European Alps during the YD-EH transition (e.g. Ilyashuk et al., 2009; Larocque-Tobler et al., 2010; Samartin et al., 2012). Concurrent with this general warming trend, moraines dating to the time period between c. 12 ka and c. 10 ka have been observed in a number of cosmogenic nuclide studies across the Alps (Baroni et al., 2017; Bichler et al., 2016; Boxleitner et al., 2019a, 2019b; Cossart et al., 2012; Hofmann et al., 2019; Ivy-Ochs et al., 2009; Kronig et al., 2018; Moran et al., 2016a, 2016b, 2017a; Protin et al., 2019; Schimmelpfennig et al., 2012, 2014, 2019; Schindelwig et al., 2012). These moraines are located outboard the LIA moraines, and inboard Late Glacial ice margins, yet at varying distances relative to the LIA moraines in both lateral and frontal sections. The presence of these moraines (or moraine sets) between Late Glacial moraines and the LIA ice margin points to several phases of glacier stabilization during an interval of general warming and glacier retreat between 12 and 10 ka (Ivy-Ochs, 2015).

In the Ochsental, ^{10}Be bedrock ages indicate ice-free conditions of Grüne Kuppe after 11 ka. We interpret the retreat of Ochsentaler and Vermunt glaciers from this section as a response to the EH warming trend. Adjacent to the sampled bedrock outcrop, GrK moraine accumulated c. 9.9 ± 0.7 ka and gives evidence for a stable glacier position during the EH. The moraine age overlaps within uncertainties with cold lapses detected in proxy records from the Alps (locations displayed in Fig. 1). A diatom record from Oberer Landschitzsee points to cooling centered around 10.2 ka (Fig. 10f), (Schmidt et al., 2006). A high-resolution oxygen isotope record from speleothems sampled at Katerloch cave exhibits a drop in δ^{18}O around 10 ka (Boch et al., 2009). Given that the timing of these climate perturbations coincides with the moraine formation interval at Grüne Kuppe, we propose a relationship between this climate anomaly, and glacier stabilization in the Ochsental.

The hypothesis of a period of cooler and wetter climate conditions in Central Europe, which has superimposed the general post-YD warming trend, was first suggested by Haas et al. (1998). The authors analyzed proxies such as pollen and macrofossils in lake sediments at four different sites on the Swiss Plateau and found evidence of vegetation changes as a response to Holocene cooling events. The onset of the Central European cold phase 1 (CE-1), the first of eight cold anomalies, occurred c. 10,500 calBP and has lasted a few hundred years. Another paleobotanical proxy record derived from lake sediments in the Swiss Alps shows a cold phase c. 11,000 to 10,150 calBP, contemporaneous with CE-1 (Tinner and Kaltenrieder, 2005). Chironomid-inferred summer temperatures reconstructed from Swiss lake sediments show a period of cooler climate conditions to c. 10,700–10,500 calBP (Heiri et al., 2003, 2004). Climatic cooling between 11 and 10 ka appears to be an Alpine-wide phenomenon also documented by a number of directly dated moraines (Fig. 10d). Moreover, evidence of synchronous EH glacier advances was recently found in West Greenland, on Baffin Island, in the French Pyrenees and in Scandinavia (Jomelli et al., 2020; Solomina et al., 2015 and references therein; Young et al., 2020), which might point to EH cooling being a hemispheric phenomenon, potentially related to a freshwater pulse in the North Atlantic region (e.g. Jennings et al., 2015; Nesje et al., 2004; Thornalley et al., 2009).

The location of GrK moraine merely 45 m outboard the subsequent LIA crest suggests that glacier margins around 10 ka and during the LIA were similar at Ochsental. Along the OcG main ridge – in its frontal and left lateral sections – two boulders yield EH ages, which overlap with the GrK moraine age within uncertainties (OcG-15-01: 10.3 ± 0.2 ka and OcG-17-16: 9.5 ± 0.2 ka). Their positions amid boulders that were deposited during the LIA suggests that the OcG main ridge is a Holocene composite moraine marking a stable terminus position which was occupied repeatedly by Ochsentaler and Vermunt glaciers during the Holocene. Due to some age scatter among boulders along the OcG main ridge, we have less confidence in the ages of OcG-15-01 and OcG-17-16 compared to the robustly dated lateral GrK moraine. However, we propose that the ages reflect a true moraine deposition interval during the EH and put forward four lines of argumentation. First, the amplitude of chironomid-inferred summer temperature variations during the Holocene and therefore the magnitude of glacier fluctuations was moderate compared to the transition from the YD to the EH (e.g. Ilyashuk et al., 2009; Ilyashuk et al., 2011; Larocque and Finsinger, 2008). We hypothesize that the termini of Ochsentaler and Vermunt glaciers retreated from their Late Glacial ice margin to the OcG main ridge along with rising temperatures during the YD-EH transition. Around 10 ka, glaciers halted at or readvanced to the position of today's OcG main ridge and formed a moraine. During the LIA and potentially also during other Holocene cold phases (possibly during the Neoglacial period suggested by a

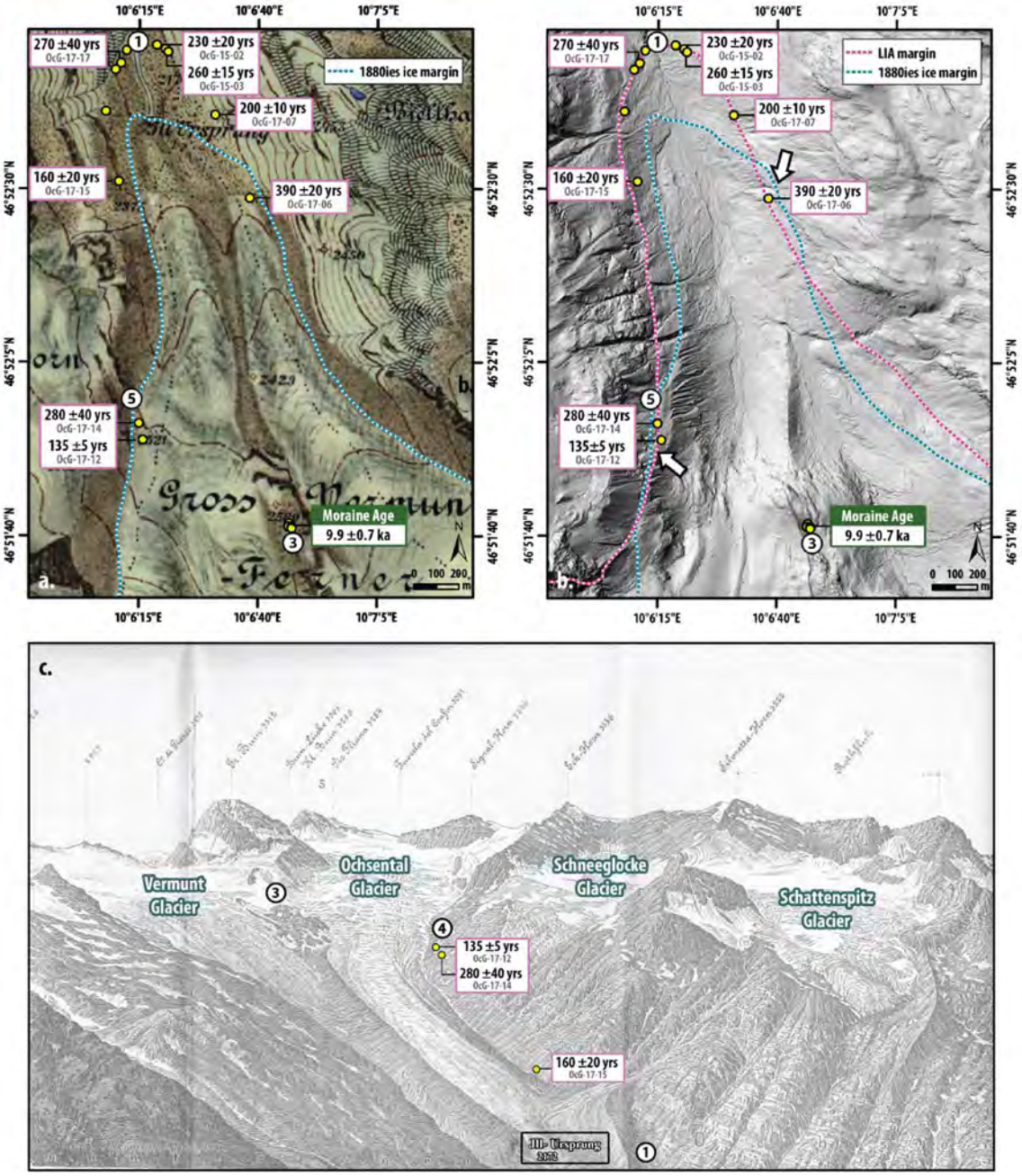

Fig. 8. Historical record. **a.** Georeferenced historical map from c. 1887 (K. u. k. Militärgeographisches Institut, 1887, Blatt 5244) with 1880s ice margin (blue dotted line). Little Ice Age (LIA) exposure ages are added to correlate the ^{10}Be data set with historical information. The latero-frontal section of the main ridge is ice-free in 1887 being consistent with LIA boulder ages. The terminus retreated c. 350–380 m from the OcG main ridge to an elevation of c. 2170–2175 m a.s.l. © BEV – 2020, N2020/73123. **b.** Digital Elevation Model (DEM) with 1880s ice margin inferred from (a.). Lateral sections in the historical map indicated by arrows are sketched inaccurately as they are outboard the moraines identified on the DEM, which is stratigraphically inconsistent. This inaccuracy explains inconsistencies between ^{10}Be boulder ages (OcG-17-06, OcG-17-12, OcG-17-14) and the 1880s ice margin. **c.** Panorama from Ochsental drawn in 1888 (Immler and von Siegl, 1888). Glacier terminus (="Ill-Usprung", black rectangle) marked at an elevation of 2172 m a.s.l., being in line with the historical map (a.). Sample positions were deduced by overlaying the drawing with a modern photograph taken from the same position (Hohes Rad). According to the ^{10}Be age, sample OcG-17-12 was exposed 135 ± 5 yrs ago corresponding to a time frame between the 1870s and 1890s, which is a plausible timing for deglaciation of this area. The ^{10}Be age of OcG-17-15 gives a central age of exposure of 160 ± 20 yrs (1857 CE ±20 years), which is in good agreement with both, the historical map (a.) and the panorama sketch (c.). (For interpretation of the references to color in this figure legend, the reader is referred to the Web version of this article.)

boulder age of 1500 ± 40 yrs along OcG main ridge), glaciers returned to the position of the OcG main ridge, but did not advance beyond it. Second, the time of exposure influences lichen colonialization on rock surfaces, i.e. boulders with exposure ages of several thousand years are expected to exhibit more developed lichen populations than boulders which were deposited some centuries (or decades) ago. This pattern is visible on the sampled boulder surfaces including OcG-15-01 and OcG-17-16 (appendix, section 5) and increases confidence in corresponding EH exposure ages. Third, in a map outlining the ice margins of Ochsental and Vermunt in the year of 1860, the glacier terminus is located at the OcG main ridge, while Grüne Kuppe is largely ice-free (Vorndran, 1968; Fig. 11). Given that during the EH, the upstream lateral GrK moraine is preserved some meters outboard the LIA

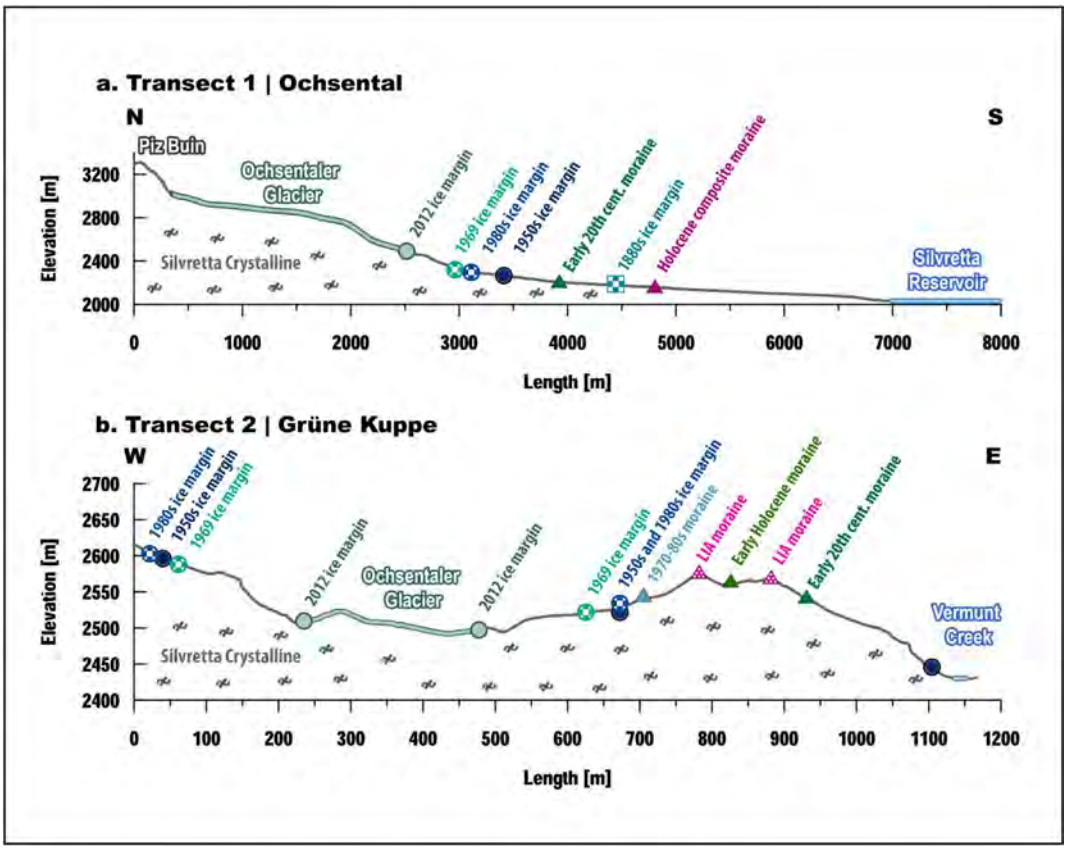

Fig. 9. Transects illustrating Holocene ice margin reconstructions in the Ochsental based on instrumental records (circles) (Fischer et al., 2015; Landesamt für Vermessung und Geoinformation, 2019), historical documents (rectangle) (Immler and von Siegl, 1888; K. u. k. Militärgeographisches Institut, 1887) and mapped moraines (triangles). Positions of the transects are shown in Fig. 2 and 3. **a.** Transect 1: N-S transect of Ochsental from Piz Buin summit to the Silvretta reservoir. **b.** Transect 2: W-E transect from left-lateral valley side via Grüne Kuppe to Vermunt creek.

ridge (and was not overprinted in the course of LIA culminations), we cannot exclude that the terminus also extended further down the valley relative to the LIA ice margin. However, we note that ice configurations during the EH and during the LIA were similar according to the Vorndran map and the new ^{10}Be chronology, which gives an indication of the order of magnitude of glacier sizes during these two periods. Fourth, we report some geomorphological details in the context of the OcG main ridge, which – albeit not quantitative – might be of interest with respect to a stable EH ice margin along the OcG main ridge. The Ill river shows a typical braided channel system at the glacier-proximal side of the OcG main ridge, whereas downstream, the river has incised several meters into gneissic bedrock (Fig. 4c). This discontinuity may indicate a stable glacier terminus over several thousands of years. According to our geochronology the glacier snout was at, or close to the position of the discontinuity around 10 ka, perhaps during the Neoglacial, and certainly during the LIA. Even though it is difficult to quantify the time required for the river to cut down this deeply into the bedrock, we estimate the cumulative duration to be in the order of thousands of years, which is consistent with our age model. Another geomorphological feature is a bedrock outcrop outboard the left latero-frontal section of the OcG main ridge, which may act as a natural barrier for Ochsentaler and Vermunt glaciers (Fig. 4c). Even though we do not have a cumulative exposure age of the outcrop, we speculate that a certain threshold of ice volume might be required to overcome this barrier, which – according to the EH ^{10}Be boulder ages along the OcG main ridge – was not reached within the last c. 10 ka.

Based on the above arguments, we assume that both EH boulders reflect a plausible moraine deposition age, with more confidence in OcG-15-01 due to is prominent pole position in the frontal section of the OcG main ridge (see sample documentation in the appendix – section 4). This assumption has two implications: First, the OcG main ridge is a Holocene composite moraine, which marks at least two phases of glacier stabilization and/or readvance during the Holocene. Second, glaciers at Ochsental had similar extents around 10 ka and during the LIA, which is corroborated by the age and position of the GrK moraine. This finding is consistent with several radiocarbon and dendrochronological records in the Eastern European Alps, which indicate peat formation and tree growth and thus ice-free conditions in the forefield of LIA moraines during the EH (Bortenschlager, 1984; Patzelt, 2015, 2016; Patzelt and Bortenschlager, 1973). Furthermore, a recent multi-proxy study on lake sediments in South Tyrol shows that a glacial lake located at an altitude of c. 2790 m a.s.l. adjacent to the LIA margin lost its connection to the local glaciers around 10 ka (Koinig et al., 2019), which is in line with the glacier chronology from Ochsental.

Interestingly, a ^{10}Be moraine record from adjacent Kromertal and Klostertal gives a somewhat different picture, suggesting that glaciers in these valleys were significantly larger around 10 ka compared to their LIA extent (Moran et al., 2016b) (Fig. 2). The discrepancy of coeval moraines indicating distinct glacier configurations in neighboring valleys can be explained by geomorphological uncertainties or uncertainties related to the ^{10}Be SED method, or by varying conditions for moraine preservation from valley to valley. Another reason for dissimilarities between the

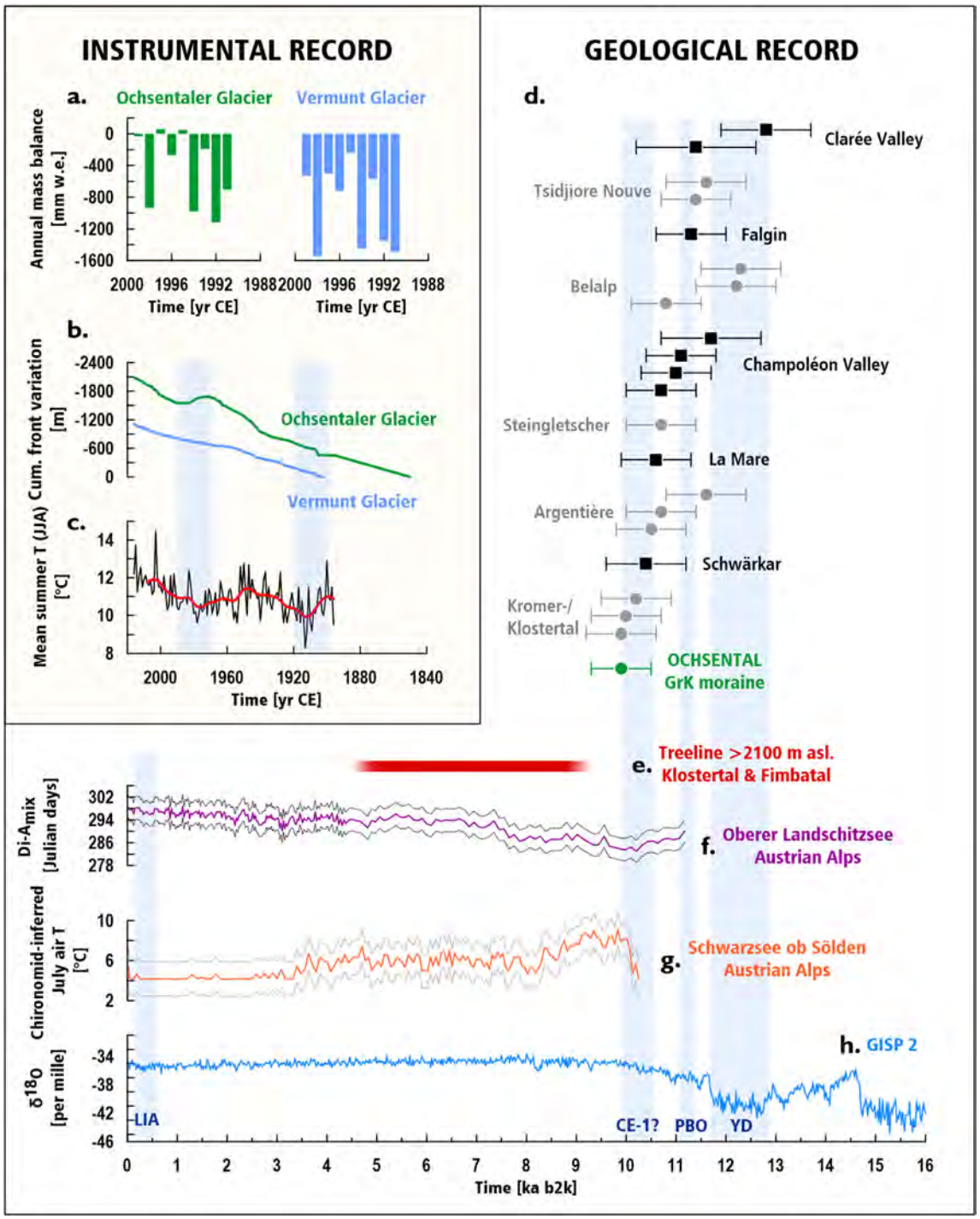

Fig. 10. Oscillations of Ochsentaler and Vermunt glaciers on geological and modern time scale put into an Alpine-wide context. Instrumental records: **a.** Mass balances of Ochsentaler and Vermunt glaciers available for the years of 1991–1999 (WGMS, 2018). **b.** Cumulative front variations of Ochsentaler glacier (1850–2016 CE) and Vermunt glacier (1903–2016 CE) (WGMS, 2018). **c.** Mean summer temperature (June-July-August) since 1896 to 2008 adopted from HISTALP (Auer et al., 2007) and time series from 2009 to 2016 based on BMNT (2019). **d.** Recalculated landform ages from Younger Dryas-Early Holocene Surface Exposure Dating (SED) studies in the European Alps. Landform ages were recalculated following the Ochsental age model (Swiss production rate, time-dependent 'Lm' scaling; appendix – section 7). Clarée Valley (Cossart et al., 2012), Tsidjiore Nouve (Schimmelpfennig et al., 2012), Falgin (Moran et al., 2016a), Belalp (Schindelwig et al., 2012), Champoléon (Hofmann et al., 2019), Steingletscher (Schimmelpfennig et al., 2014), La Mare (Baroni et al., 2017), Argentière (Protin et al., 2019), Schwärkar (Moran et al., 2017a), Kromer- and Klostertal (Moran et al., 2016b). Ochsental – GrK moraine subject of this study. **e.** Subfossil tree record from Klostertal and Fimbatal indicating treeline above 2100 m a.s.l. (Nicolussi, 2010). **f.** Diatom record from Oberer Landschitzsee in the Austrian Alps (Schladminger Tauern): Minimum from c. 9.5 to 10.5 ka indicates cooler and wetter climate conditions (Schmidt et al., 2006) and coincides with the Central European cooling period (CE-1) (Haas et al., 1998). **g.** Chironimid-inferred July air temperature from Schwarzsee ob Sölden in Tyrol, Austria (Ötztal) (Ilyashuk et al., 2011) indicating a cool period coinciding with moraine formation in the Ochsental (GrK moraine). **h.** $\delta^{18}O$ in Greenland ice core GISP 2 (Rasmussen et al., 2006).

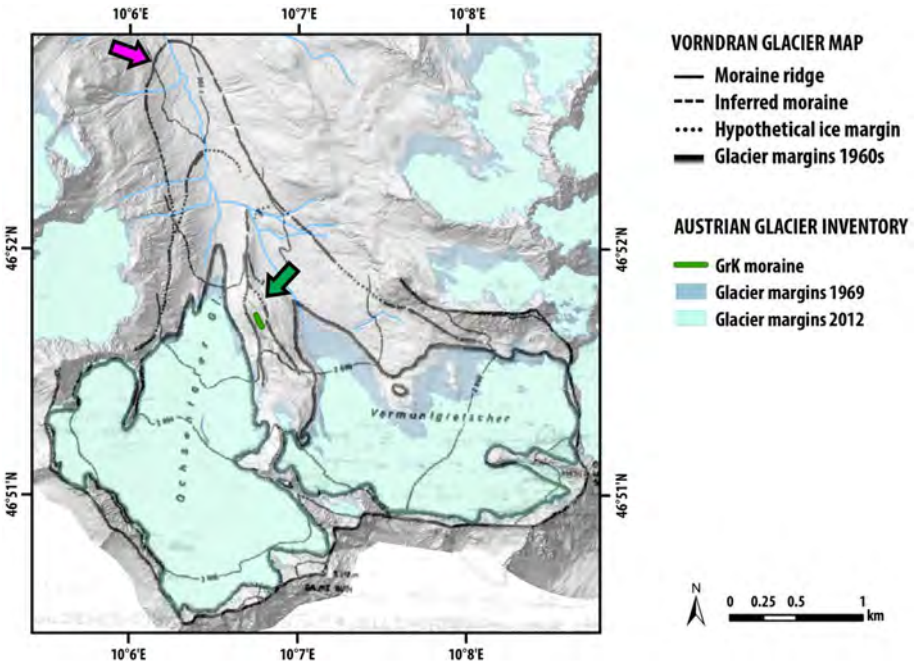

Fig. 11. Compilation of glacier map by Vorndran (1968) and ice margins from the Austrian Glacier Inventory (Fischer et al., 2015). The map depicts glacier configurations at the very end of the Little Ice Age (LIA). According to Vorndran (1968), the ice margin around 1860 CE is located at the OcG main ridge position (pink arrow), while Grüne Kuppe (GrK moraine in green) is ice-free (green arrow), which is confirmed by EH ^{10}Be bedrock and boulder ages from this site. This glacier configuration resembles ice margins suggested by the new ^{10}Be chronology and makes a case for Ochsentaler and Vermunt glaciers having approximately the same size around 10 ka and the LIA. The consistency between the Vordran map and the ^{10}Be record suggests an update of the AGI, in which Grüne Kuppe is displayed as ice-covered during the LIA (Fig. 2). (For interpretation of the references to color in this figure legend, the reader is referred to the Web version of this article.)

records could be different glacier responses in the catchments, for instance due to local bed topography, distinct shading situations or glacier hypsometry (e.g. Strelin et al., 2014). One potential way to reconcile results from the Kromer- and Klostertal with results presented in this study is the systematic modeling of Equilibrium Line Altitudes (ELAs), which will be subject of future work.

6.2. Mid-Holocene

According to a trend observed in numerous different paleoclimate proxies, climate in the European Alps underwent a transition towards warmer temperatures in the time period between c. 10 ka and c. 5 ka (e.g. Ivy-Ochs et al., 2009 and references therein; Joerin et al., 2006; Luetscher et al., 2011; Nicolussi et al., 2005; Nicolussi and Patzelt, 2001; Solomina et al., 2015, and references therein). Mid-Holocene climate conditions prompted glaciers to recede to sizes smaller than today over extended periods of time (e.g. Goehring et al., 2011; Hormes et al., 2001; Joerin et al., 2008). This pattern of glacier retreat is consistent with high treelines during the Mid-Holocene documented at Klostertal and Fimbatal in the Silvretta region. Nicolussi (2010) calendar-dated subfossil tree logs recovered at Klostertal at elevations of c. 2125–2200 m a.s.l. (Fig. 2). The record makes a case for the paleo-treeline being c. 100–200 m above the maximum treeline elevation typical for the 20th century. Trees above the modern timberline were growing as early as c. 9320 calBP (7370 calBC) until 4535 calBP (2585 calBC) at Klostertal, implying ice-free conditions during this time period inboard the Kromer moraine (Figs. 2 and 10e). Dendrochronological data in combination with radiocarbon ages from Fimbatal located c. 20 km SE of Ochsental paint a similar picture with tree logs found at even higher elevations (2200–2360 m a.s.l.), yielding ages of c. 8480 calBP (6530 calBC) to 6690 calBP (4740 calBC) (Nicolussi, 2010; Remy, 2012). These findings are consistent with geochronological and palynological results gained from a peat core drilled at Fimbatal adjacent to the site where subfossil wood samples were found (Dietre et al., 2014). The core reaching back to 10,400 calBP shows pollen assemblages, which indicate an open forest with extensive stands of Pinus cembra above 2370 m a.s.l. from c. 10,400 to 5000 calBP.

Warm climate conditions in the Silvretta region during the Mid-Holocene are corroborated by archeological evidence. Shrinking glaciers allowed passage across mountain chains, which were glaciated during the YD and the EH. Evidence of fireplaces as well as tools and arrowheads found on both, the north- and south-oriented side of the Silvretta Massif at elevations between 2000 and 2500 m a.s.l. point to human presence at high altitudes as early as c. 10,580 calBP (8630 calBC), although the majority of artifacts dates to c. 8450 calBC (6500 calBC) and younger (Reitmaier, 2012; Reitmaier and Walser, 2016). Throughout the Holocene Thermal Optimum, human impact along the timberline increased, which is reflected in charcoal horizons found in soil profiles and peat cores, and changes in pollen assemblages indicating pasture and grazing at high elevation sites at Fimbatal (Dietre et al., 2014). In parallel to climatic and environmental changes during the Mid-Holocene, a shift of subsistence strategies from hunting to herding is estimated to c. 4800 to 4500 calBP in the Silvretta Massif (Dietre et al., 2020; Kothieringer et al., 2015).

Our review of complementary paleoclimate studies makes a strong case for Silvretta glaciers having been smaller than today during the Mid-Holocene, which is consistent with comparable studies across the European Alps (e.g. Badino et al., 2018; Bonani et al., 1994; Festi et al., 2014; Hafner, 2012; Joerin et al., 2006; Nicolussi et al., 2005; Nicolussi and Patzelt, 2001; Spindler, 1994).

6.3. Neoglacial period

At the onset of the Neoglacial cooling period c. 5 ka (Deline and Orombelli, 2005; Haas et al., 1998; Luetscher et al., 2011; Magny et al., 2009; Simonneau et al., 2014), glaciers in the European Alps became more active again (Grove, 2004; Ivy-Ochs et al., 2009; Luetscher et al., 2011; Solomina et al., 2015, and references therein). Even though the onset of the Neoglacial cooling appears to be variable across time and space, calendar dated subfossil wood found in moraine deposits of Gepatschferner and of Mer de Glace provide strong evidence for the glaciers advancing during the 17th and 16th century BC (Le Roy et al., 2015; Nicolussi and Patzelt, 2001), which is consistent with the timing of the Löbben oscillation postulated by Patzelt and Bortenschlager (1973). Recently published moraine chronologies and proxy studies are in agreement with this timing and indicate glacier growth around 3.8 to 3.4 ka (Badino et al., 2018; Le Roy et al., 2017; Moran et al., 2017b; Schimmelpfennig et al., 2012). Due to the inherent incompleteness of moraine records, this climate perturbation is not preserved in Ochsental's geomorphology. Moraine deposits older than the LIA and younger than the EH were likely removed by LIA advances or are incorporated in the LIA ridge. However, a boulder age of 1500 ± 40 yrs (OcG-15-04) along the OcG main ridge coincides with a cool climate episode, when summer temperatures across Europe were below the average of the past 2500 years (Büntgen et al., 2011, 2016). The boulder age is also consistent with glacier culminations detected in other parts of the Alps (Holzhauser et al., 2005; Kronig et al., 2018; Le Roy et al., 2015; Wipf, 2001), which allows speculations about glaciers at Ochsental readvancing to the OcG main ridge around 1500 yrs ago (c. 500 CE).

6.4. Little Ice Age (LIA)

Historical exposure ages at Ochsental show that glaciers reached the OcG main ridge, during this most recent cold lapse. Youngest boulder ages inboard the OcG main ridge overlap with the historical record, which allows us to test the robustness of the Ochsental ^{10}Be moraine chronology.

In two consistent historical sources from the 1880s, the glacier terminus is depicted at an elevation of c. 2170–2175 m a.s.l., ca. 350–380 m inboard the OcG main ridge, while Grüne Kuppe is not glaciated (Fig. 8). Hence, we consider the glacier's terminus position and ice-free conditions at Grüne Kuppe at that time as reliable information. Along the latero-frontal sections of the OcG main ridge, all exposure ages are older than 200 yrs (1817 CE), which is in line with the retreated 1880s ice-margin in both, the map and the sketch. Boulder OcG-17-15 located inboard the OcG main ridge, but outboard the 1880s ice margin, dates to 160 ± 20 yrs (c. 1857 CE ±20 yrs) and is in good agreement with the retreated and lowered ice margin in the 1880s (Fig. 8a and c). The consistency among historical sources and the ^{10}Be record highlights that inheritance had no significant effect on the historic ^{10}Be age group and is, if present, limited to a few decades.

While configurations of the glacier terminus and the Grüne Kuppe section in the sketch and the map are convincing, we have less confidence in lateral ice margin positions. In sections, where exposure ages are inconsistent with the historical (1880s) ice margin in the map (OcG-17-06, OcG-17-12 and OcG-17-14), the latter is located outboard the OcG moraine ridge, which is stratigraphically impossible (Fig. 8b). However, exposure ages in these sections are consistent with ice margins in the panorama sketch and are in stratigraphic order (OcG-17-12 and OcG-17-14) (Fig. 8c). We hence argue that ^{10}Be exposure ages are realistic estimates for moraine deposition in these sections.

Four historical ^{10}Be ages (OcG-15-02, OcG-15-03, OcG-17-14 and OcG-17-17) indicate a glacier advance in the mid to late 18th century. Chironomid-inferred summer temperature reconstructions from glacial lake sediments in the Stubai Alps (Schwarzsee ob Sölden, Fig. 1), c. 80 km East of Ochsental, indicate a cooling during the 18th century with a temperature minimum of 1.5 °C below the long-term mean from 1300 to 2000 CE during the 1780s (Ilyashuk et al., 2019). This period coincides with cold peaks in complementary temperature proxies (e.g. Corona et al., 2010; Esper et al., 2007; Osborn and Briffa, 2006) and homogenized temperature time series from the Austrian Alps (Böhm et al., 2001). Also, glaciers at Zemmgrund in the Zillertal Alps, and Vernagtferner in the Ötztal Alps – located close to the Stubai Alps and Ochsental – advanced during this LIA cold peak (Nicolussi, 2013; Pindur and Heuberger, 2010). We propose that the clustering of LIA boulder ages in the Ochsental represents the response of Ochsental and Vermunt glaciers to the temperature drop during the 18th century. One boulder age along the OcG main ridge pre-dates this cluster (OcG-17-06: 390 ± 20 yrs) and possibly points to an earlier culmination of Ochsentaler and Vermunt glaciers, concurrent with advances of other Austrian glaciers such as Gepatschferner and Pasterze (Nicolussi and Patzelt, 2001).

In summary, the LIA ^{10}Be record suggests that glaciers in the Ochsental have come close to their EH moraine during the mid to late 18th century, and perhaps also during the 17th century and the early 19th century. The LIA ice margin marked by the OcG main ridge is constrained by eight ^{10}Be ages, it is consistent with geomorphological observations and it is in line with results from preceding mapping campaigns (Fischer et al., 2015; Hertl, 2001; Vorndran, 1968). A cross-check between the youngest ^{10}Be exposure ages and historical documents supports the validity of these ages and shows that inheritance of ^{10}Be is negligible in the Ochsental samples.

7. Summary and conclusions

The glacier chronology from Ochsental in the Silvretta Massif in Austria compiles information on glacier fluctuations as a response to climate change throughout the Holocene. Four different types of records were synthesized in order to link the geological with the modern time scale: (i) a new ^{10}Be moraine record, (ii) pre-existing complementary paleoclimate proxy records, (iii) historical documents, and (iv) instrumental time series on glacier variations and temperature change.

i. Our new cosmogenic nuclide moraine chronology comprises the first ^{10}Be exposure ages of LIA glacier culminations in the Austrian Alps and includes some of the youngest ^{10}Be ages in the European Alps. Results indicate that glaciers in the Ochsental stabilized during the EH and had similar ice margin configurations during the LIA.
ii. An evaluation of complementary climate proxy records suggests that the treeline in the Silvretta Massif was above 2100 m a.s.l. (or higher) during the Mid-Holocene, implying that glaciers had retreated to higher elevations between c. 10 ka and 5 ka.
iii. Historical documents show that glaciers in the Ochsental had retreated from their LIA maximum c. 350 m inboard the Holocene composite moraine in the 1880s. During the early 20th century, a brief cold lapse led to the stabilization of Ochsentaler glacier, evidenced by moraine formation c. 800 m inboard the Holocene composite moraine (OcG main ridge).
iv. Instrumental time series on glacier extents and mass balance changes were correlated with temperature series and highlight the rapidity of modern glacier change along with

increasing atmospheric temperatures. Glaciers in the Ochsental were steadily retreating since the end of the LIA with two exceptions, the early 20th century and in the 1970s and 1980s, paralleling temperature minima in the temperature record. On average, Ochsentaler and Vermunt glaciers retreated 17 and 19 m/yr within the past 10 years.

Finally, we address the objectives of this study by answering the following questions:

1. ***Are the timing and magnitude of Holocene glacier advances in the Ochsental comparable to the Central and Western Alps?***

Glaciers across the European Alps retreated from their Late Glacial extent between c. 12 and 10 ka, responding to warming temperatures during the transition from the YD to the EH. In several Alpine valleys, moraines between the LIA and the YD ice margin are identified, which document phases of glacier stabilization and punctuations of the general warming trend. The GrK moraine in the Ochsental yields an age of 9.9 ± 0.7 ka and is interpreted as geomorphological expression of an EH cold snap between c. 10.5 and 10 ka, the CE-1 detected in a number of proxy records across the Alps. The age of the GrK moraine in combination with the ^{10}Be LIA ages suggest that glaciers in the Ochsental had similar configurations around 10 ka and during LIA. This finding is consistent with several paleoenvironmental studies in the Alps, which suggest that glaciers have retreated within the LIA margin around 10 ka. ^{10}Be moraine chronologies from the adjacent Kromertal and Klostertal indicate that glaciers were in advanced positions relative to the LIA margin around 10 ka. Discrepancies among the Ochsental record presented in this study and the Kromer- and Klostertal records may be caused by geomorphological and/or dating uncertainties, or could be explained by different glacier response times, which may be attributed to the influence of local factors such as bed topography, shading, or debris cover, or a combination of all three points. The application of a comparative ELA model across the Silvretta region, which will be subject of future work, will help to test these hypotheses and will increase our understanding of glacier responses to climate change in the region, and beyond.

2. ***Is ^{10}Be SED apt for dating LIA deposits and for detecting the fine structure of LIA culminations?***

LIA exposure ages are stratigraphically consistent and suggest multi-phased glacier advances in the Ochsental with strong evidence of a culmination in the 18th century. This time period coincides with a temperature minimum in paleoclimate proxy records from the Austrian Alps and is synchronous with well-documented advances of other glaciers in the Austrian Alps

3. ***Are the youngest ^{10}Be ages consistent with historical records?***

The late 19th century and early 20th century are challenging to capture with ^{10}Be exposure due to limits inherent to the dating method. However, in the European Alps, systematic recording of glacier and meteorological data goes back many decades and begins in the second half of 19th century in the Silvretta Massif. The overlap of these meteorological time series and other historical sources with historical ^{10}Be ages of the Ochsental record provides a unique opportunity to test the robustness of these ages independently. The youngest ^{10}Be ages of the Ochsental record (central age ≤160 yrs) are in good agreement with historical documents and indicate that there is no significant signal of pre-exposure in the historical samples.

Credit author statement

Sandra M. Braumann: Conceptualization, Data Curation, Field work, Sample processing, Funding acquisition, Investigation, Project administration, Visualization, Writing - Original Draft, Writing - Review & Editing; Joerg M. Schaefer: Conceptualization, Field work, Resources, Supervision, Writing - Review & Editing; Stephanie M. Neuhuber: Field work, Resources, Writing - Review & Editing; Jürgen M. Reitner: Field work, Writing - Review & Editing; Christopher Lüthgens: Field work, Writing - Review & Editing; Markus Fiebig: Field work, Funding acquisition, Resources, Supervision, Writing - Review & Editing.

Declaration of competing interest

The authors declare that they have no known competing financial interests or personal relationships that could have appeared to influence the work reported in this paper.

Acknowledgements

The authors thank inatura Erlebnis Naturschau GmbH Dornbirn for generously sponsoring this study. SMB is a recipient of a DOC Fellowship of the Austrian Academy of Sciences (OeAW) at the Institute of Applied Geology, University of Natural Resources and Life Sciences (BOKU) Vienna. For research visits at the Lamont-Doherty Earth Observatory (LDEO), SMB received a Marietta Blau Scholarship sponsored by OeAD GmbH, a Marshall Plan Scholarship provided by the Austrian Marshall Plan Foundation and financial support from BOKU's 'Transitions to Sustainability' (T2S) doctoral school. SMB is grateful to the LDEO Cosmogenic Isotope Group, in particular R. Schwartz, J. Hanley and J. Frisch for help with ^{10}Be sample processing and M. Kaplan for his expertise with the manuscript. The authors acknowledge M. Bichler and E. Rades for assistance in the field and S. Zimmerman and A. Hidy from the Center for Accelerator Mass Spetrometry (CAMS) at Lawrence Livermore National Laboratory (LLNL) for sample analyses. We thank G. Gross for discussing Holocene glacier evolution in the Ochsental and the staff of Wiesbadener Hütte and Pension Türtscher for facilitating field work. Finally, we would like to express our gratitude to two anonymous reviewers whose valuable comments have greatly improved the manuscript.

Appendix A. Supplementary data

Supplementary data to this article can be found online at https://doi.org/10.1016/j.quascirev.2020.106493.

References

Alley, R.B., 2000. The Younger Dryas cold interval as viewed from central Greenland. Quat. Sci. Rev. 19, 213–226. https://doi.org/10.1016/S0277-3791(99)00062-1.

André, M.F., 2002. Rates of postglacial rock weathering on glacially scoured outcrops (Abisko-Riksgransen area, 68 degrees N). Geogr. Ann. 84a, 139–150. https://doi.org/10.1111/j.0435-3676.2002.00168.x.

Auer, I., Böhm, R., Jurkovic, A., Lipa, W., Orlik, A., Potzmann, R., Schöner, W., Ungersböck, M., Matulla, C., Briffa, K., Jones, P., Efthymiadis, D., Brunetti, M., Nanni, T., Maugeri, M., Mercalli, L., Mestre, O., Moisselin, J.M., Begert, M., Müller-Westermeier, G., Kveton, V., Bochnicek, O., Stastny, P., Lapin, M., Szalai, S., Szentimrey, T., Cegnar, T., Dolinar, M., Gajic-Capka, M., Zaninovic, K., Majstorovic, Z., Nieplova, E., 2007. HISTALP – Historical instrumental climatological surface time series of the Greater Alpine Region. Int. J. Climatol. 27, 17–46. https://doi.org/10.1002/joc.1377.

Badino, F., Ravazzi, C., Vallè, F., Pini, R., Aceti, A., Brunetti, M., Champvillair, E., Maggi, V., Maspero, F., Perego, R., Orombelli, G., 2018. 8800 years of high-altitude vegetation and climate history at the Rutor Glacier forefield, Italian Alps – Evidence of middle Holocene timberline rise and glacier contraction. Quat. Sci. Rev. 185, 41–68. https://doi.org/10.1016/j.quascirev.2018.01.022.

Balco, G., 2011. Contributions and unrealized potential contributions of cosmogenic-

nuclide exposure dating to glacier chronology, 1990-2010. Quat. Sci. Rev. 30 (1–2), 3–27. https://doi.org/10.1016/j.quascirev.2010.11.003.
Balco, G., Briner, J., Finkel, R.C., Rayburn, J.A., Ridge, J.C., Schaefer, J.M., 2009. Regional beryllium-10 production rate calibration for late-glacial northeastern North America. Quat. Geochronol. 4, 93–107. https://doi.org/10.1016/j.quageo.2008.09.001.
Baroni, C., Casale, S., Salvatore, M.C., Ivy-Ochs, S., Christl, M., Carturan, L., Seppi, R., Carton, A., 2017. Double response of glaciers in the upper PeioValley (Rhaetian Alps, Italy) to the younger Dryas climatic deterioration. Boreas 46 (4), 783–798. https://doi.org/10.1111/bor.12284.
Bertle, H., 1973. Zur Geologie des Fensters von Gargellen (Vorarlberg) und seines Kristallinen Rahmens – Österreich, 22. Mitt. Ges. Geol. Bergbaustd., Wien, pp. 1–60.
Bichler, M.G., Reindl, M., Reitner, J.M., Drescher-Schneider, R., Wirsig, C., Christl, M., Hajdas, I., Ivy-Ochs, S., 2016. Landslide deposits as stratigraphical markers for a sequence-based glacial stratigraphy: a case study of a Younger Dryas system in the Eastern Alps. Boreas 45 (3), 537–551. https://doi.org/10.1111/bor.12173.
Blunden, J., Arndt, D.S., 2019. State of the Climate in 2018. Bull. Amer. Meteor. Soc. 100 (9).
BMNT, 2016. Hydrographisches Jahrbuch von Österreich. Federal Minstry for Sustainability and Tourism, Vienna.
BMNT, 2018. Energie in Österreich 2018. Federal Minstry for Sustainability and Tourism, p. 36. Vienna.
BMNT, 2019. eHYD. BMNT, Vienna.
Boch, R., Spötl, C., Kramers, J., 2009. High-resolution isotope records of early Holocene rapid climate change from two coeval stalagmites of Katerloch Cave, Austria. Quat. Sci. Rev. 28, 2527–2538. https://doi.org/10.1016/j.quascirev.2009.05.015.
Böhm, R., Auer, I., Brunetti, M., Maugeri, M., Nanni, T., Schöner, W., 2001. Regional temperature variability in the European Alps: 1760-1998 from homogenized instrumental time series. Int. J. Climatol. 21 (14), 1779–1801. https://doi.org/10.1002/joc.689.
Bonani, G., Ivy, S.D., Hajdas, I., Niklaus, T.R., Suter, M., 1994. AMS C-14 Age-determinations of tissue, bone and grass samples from the Ötztal Ice Man. Radiocarbon 36 (2), 247–250. https://doi.org/10.1017/S0033822200040534.
Borchers, B., Marrero, S., Balco, G., Caffee, M., Goehring, B., Lifton, N., Nishiizumi, K., Phillips, F., Schaefer, J., Stone, J., 2016. Geological calibration of spallation production rates in the CRONUS-Earth project. Quat. Geochronol. 31, 188–198. https://doi.org/10.1016/j.quageo.2015.01.009.
Bortenschlager, S., 1984. Beiträge zur Vegetationsgeschichte Tirols I. Inneres Ötztal und unteres Inntal. Ber. Nat. Med. Verein Innsbruck 71, 19–56.
Boxleitner, M., Ivy-Ochs, S., Egli, M., Brandova, D., Christl, M., Dahms, D., Maisch, M., 2019a. The 10Be deglaciation chronology of the Göschenertal, central Swiss Alps, and new insights into the Göschenen Cold Phases. Boreas. https://doi.org/10.1111/bor.12394.
Boxleitner, M., Ivy-Ochs, S., Egli, M., Brandova, D., Christl, M., Maisch, M., 2019b. Lateglacial and early Holocene glacier stages – new dating evidence from the Meiental in central Switzerland. Geomorphology 340, 15–31. https://doi.org/10.1016/j.geomorph.2019.04.004.
Brunner, M.I., Farinotti, D., Zekollari, H., Huss, M., Zappa, M., 2019. Future shifts in extreme flow regimes in Alpine regions. Hydrol. Earth Syst. Sci. 23, 4471–4489. https://doi.org/10.5194/hess-23-4471-2019.
Buntgen, U., Myglan, V.S., Ljungqvist, F.C., McCormick, M., Di Cosmo, N., Sigl, M., Jungclaus, J., Wagner, S., Krusic, P.J., Esper, J., Kaplan, J.O., de Vaan, M.A.C., Luterbacher, J., Wacker, L., Tegel, W., Kirdyanov, A.V., 2016. Cooling and societal change during the late antique little ice age from 536 to around 660 AD. Nat. Geosci. 9, 231–236. https://doi.org/10.1038/Ngeo2652.
Büntgen, U., Tegel, W., Nicolussi, K., McCormick, M., Frank, D., Trouet, V., Kaplan, J.O., Herzig, F., Heussner, K.U., Wanner, H., Luterbacher, J., Esper, J., 2011. 2500 Years of European climate variability and human susceptibility. Science 331, 578–582. https://doi.org/10.1126/science.1197175.
Claude, A., Ivy-Ochs, S., Kober, F., Antognini, M., Salcher, B., Kubik, P.W., 2014. The Chironico landslide (Valle Leventina, southern Swiss Alps): age and evolution. Swiss J. Geosci. 107, 273–291. https://doi.org/10.1007/s00015-014-0170-z.
Corona, C., Guiot, J., Edouard, J.L., Chalié, F., Büntgen, U., Nola, P., Urbinati, C., 2010. Millennium-long summer temperature variations in the European Alps as reconstructed from tree rings. Clim. Past 6, 379–400. https://doi.org/10.5194/cp-6-379-2010.
Cossart, E., Fort, M., Bourlès, D., Braucher, R., Perrier, R., Siame, L., 2012. Deglaciation pattern during the Lateglacial/Holocene transition in the southern French Alps. Chronological data and geographical reconstruction from the Claree Valley (upper Durance catchment, southeastern France). Palaeogeogr. Palaecol. 315, 109–123. https://doi.org/10.1016/j.palaeo.2011.11.017.
Darnault, R., Rolland, Y., Braucher, R., Bourlès, D., Revel, M., Sanchez, G., Bouissou, S., 2012. Timing of the last deglaciation revealed by receding glaciers at the Alpine-scale: impact on mountain geomorphology. Quat. Sci. Rev. 31, 127–142. https://doi.org/10.1016/j.quascirev.2011.10.019.
Deline, P., Orombelli, G., 2005. Glacier fluctuations in the western Alps during the Neoglacial, as indicated by the Miage morainic amphitheatre (Mont Blanc massif, Italy). Boreas 34, 456–467. https://doi.org/10.1080/03009480500231369.
Dielforder, A., Hetzel, R., 2014. The deglaciation history of the Simplon region (southern Swiss Alps) constrained by Be-10 exposure dating of ice-molded bedrock surfaces. Quat. Sci. Rev. 84, 26–38. https://doi.org/10.1016/j.quascirev.2013.11.008.
Dietre, B., Reitmaier, T., Walser, C., Warnk, T., Unkel, I., Hajdas, I., Lambers, K., Reidl, D., Haas, J.N., 2020. Steady transformation of primeval forest into subalpine pasture during the late neolithic to early bronze age (2300–1700 BC) in the Silvretta Alps, Switzerland. Holocene 30 (3), 355–368. https://doi.org/10.1177/0959683619887419.
Dietre, B., Walser, C., Lambers, K., Reitmaier, T., Hajdas, I., Haas, J.N., 2014. Palaeoecological evidence for Mesolithic to Medieval climatic change and anthropogenic impact on the Alpine flora and vegetation of the Silvretta Massif (Switzerland/Austria). Quat. Int. 353, 3–16. https://doi.org/10.1016/j.quaint.2014.05.001.
Dirnböck, T., Essl, F., Rabitsch, W., 2011. Disproportional risk for habitat loss of high-altitude endemic species under climate change. Global Change Biol. 17, 990–996. https://doi.org/10.1111/j.1365-2486.2010.02266.x.
EEA, 2009. Regional Climate Change and Adaptation – The Alps Facing the Challenge of Changing Water Resources. European Environment Agency, Copenhagen, p. 143.
Esper, J., Büntgen, U., Frank, D., Pichler, T., Nicolussi, K., 2007. Updating the Tyrol tree-ring dataset. Tree Rings Archaeol. Climatol. Ecol. (TRACE) 5, 80–85.
Farinotti, D., Usselmann, S., Huss, M., Bauder, A., Funk, M., 2012. Runoff evolution in the Swiss Alps: projections for selected high-alpine catchments based on ENSEMBLES scenarios. Hydrol. Process. 26, 1909–1924. https://doi.org/10.1002/hyp.8276.
Federici, P.R., Granger, D.E., Pappalardo, M., Ribolini, A., Spagnolo, M., Cyr, A.J., 2008. Exposure age dating and Equilibrium line altitude reconstruction of an Egesen moraine in the Maritime Alps, Italy. Boreas 37 (2), 245–253. https://doi.org/10.1111/j.1502-3885.2007.00018.x.
Fenton, C.R., Hermanns, R.L., Blikra, L.H., Kubik, P.W., Bryant, C., Niedermann, S., Meixner, A., Goethals, M.M., 2011. Regional Be-10 production rate calibration for the past 12 ka deduced from the radiocarbon-dated Grotlandsura and Russenes rock avalanches at 69 degrees N, Norway. Quat. Geochronol. 6, 437–452. https://doi.org/10.1016/j.quageo.2011.04.005.
Festi, D., Putzer, A., Oeggl, K., 2014. Mid and late Holocene land-use changes in the Ötztal Alps, territory of the neolithic iceman "Ötzi". Quat. Int. 353, 17–33. https://doi.org/10.1016/j.quaint.2013.07.052.
Festi, D., Hoffmann, D.L., Luetscher, M., 2016. Pollen from accurately dated speleothems supports alpine glacier low-stands during the early Holocene. Quat. Res. 86 (1), 45–53. https://doi.org/10.1016/j.yqres.2016.05.003.
Fischer, A., Seiser, B., Waldhuber, M.S., Mitterer, C., Abermann, J., 2015. Tracing glacier changes in Austria from the Little Ice Age to the present using a lidar-based high-resolution glacier inventory in Austria. Cryosphere 9, 753–766. https://doi.org/10.5194/tc-9-753-2015.
Fuchs, G., Oberhauser, R., 1990. 170 Galtür. Geologische Bundesanstalt, Vienna.
Gobiet, A., Kotlarski, S., Beniston, M., Heinrich, G., Rajczak, J., Stoffel, M., 2014. 21st century climate change in the European Alps – A review. Sci. Total Environ. 493, 1138–1151. https://doi.org/10.1016/j.scitotenv.2013.07.050.
Goehring, B.M., Schaefer, J.M., Schlüchter, C., Lifton, N.A., Finkel, R.C., Jull, A.J.T., Akçar, N., Alley, R.B., 2011. The Rhone Glacier was smaller than today for most of the Holocene. Geology 39 (7), 679–682. https://doi.org/10.1130/G32145.1.
Gosse, J.C., Phillips, F.M., 2001. Terrestrial in situ cosmogenic nuclides: theory and application. Quat. Sci. Rev. 20 (14), 1475–1560. https://doi.org/10.1016/S0277-3791(00)00171-2.
Gross, G., 2015. Gletscher- und Klimaentwicklung rund um den Piz Buin. In: Kasper, M. (Ed.), Mythos Piz Buin – Kulturgeschichte eines Berges. Haymon Verlag, Innsbruck-Wien.
Gross, G., Kerschner, H., Patzelt, G., 1978. Methodische Untersuchungen über die Schneegrenze in den alpinen Gletschergebieten. Zeitschrift für Gletscherkunde und Glaziogeologie 12, 223–251.
Grove, J.M., 2004. Little Ice Ages : Ancient and Modern, second ed. Routledge, London ; New York.
Haas, J.N., Richoz, I., Tinner, W., Wick, L., 1998. Synchronous Holocene climatic oscillations recorded on the Swiss Plateau and at timberline in the Alps. Holocene 8 (3), 301–309. https://doi.org/10.1191/095968398675491173.
Haeberli, W., Hoelzle, M., Paul, F., Zemp, M., 2007. Integrated monitoring of mountain glaciers as key indicators of global climate change: the European Alps. Ann. Glaciol. Ser. 46, 150–160. https://doi.org/10.3189/172756407782871512.
Hafner, A., 2012. Archaeological discoveries on Schnidejoch and at other ice sites in the European Alps. Arctic 65, 189–202.
Hebenstreit, R., Ivy-Ochs, S., Kubik, P.W., Schlüchter, C., Bose, M., 2011. Lateglacial and early Holocene surface exposure ages of glacial boulders in the Taiwanese high mountain range. Quat. Sci. Rev. 30, 298–311. https://doi.org/10.1016/j.quascirev.2010.11.002.
Heiri, O., Wick, L., van Leeuwen, J.F.N., van der Knaap, W.O., Lotter, A.F., 2003. Holocene tree immigration and the chironomid fauna of a small Swiss subalpine lake (Hinterburgsee, 1515 m asl). Palaeogeogr. Palaecol. 189 (1–2), 35–53. https://doi.org/10.1016/S0031-0182(02)00592-8.
Heiri, O., Tinner, W., Lotter, A.F., 2004. Evidence for cooler European summers during periods of changing meltwater flux to the North Atlantic. PNAS 101, 15285–15288. https://doi.org/10.1073/pnas.0406594101.
Heiri, O., Koinig, K.A., Spötl, C., Barrett, S., Brauer, A., Drescher-Schneider, R., Gaar, D., Ivy-Ochs, S., Kerschner, H., Luetscher, M., Moran, A., Nicolussi, K., Preusser, F., Schmidt, R., Schoeneich, P., Schwörer, C., Sprafke, T., Terhorst, B., Tinner, W., 2014. Palaeoclimate records 60–8 ka in the Austrian and Swiss Alps and their forelands. Quat. Sci. Rev. 106, 186–205. https://doi.org/10.1016/j.quascirev.2014.05.021.

Hertl, A., 2001. Untersuchungen zur spätglazialen Gletscher- und Klimageschichte der Österreichischen Silvrettagruppe. Leopold-Franzens-Universität Innsbruck, Innsbruck, p. 265.
Hippe, K., Ivy-Ochs, S., Kober, F., Zasadni, J., Wieler, R., Wacker, L., Kubik, P.W., Schlüchter, C., 2014. Chronology of Lateglacial ice flow reorganization and deglaciation in the Gotthard Pass area, Central Swiss Alps, based on cosmogenic Be-10 and in situ C-14. Quat. Geochronol. 19, 14–26. https://doi.org/10.1016/j.quageo.2013.03.003.
Hofmann, F.M., Alexanderson, H., Schoeneich, P., Mertes, J.R., Léanni, L., ASTER Team, 2019. Post-Last Glacial Maximum glacier fluctuations in the southern Écrins massif (westernmost Alps): insights from ^{10}Be cosmic ray exposure dating. Boreas 48 (4), 1019–1041. https://doi.org/10.1111/bor.12405.
Holzhauser, H., Magny, M., Zumbühl, H.J., 2005. Glacier and lake-level variations in west-central Europe over the last 3500 years. Holocene 15, 789–801. https://doi.org/10.1191/0959683605hl853ra.
Hormes, A., Müller, B.U., Schlüchter, C., 2001. The Alps with little ice: evidence for eight Holocene phases of reduced glacier extent in the Central Swiss Alps. Holocene 11, 255–265. https://doi.org/10.1191/095968301675275728.
Ilyashuk, B., Gobet, E., Heiri, O., Lotter, A.F., van Leeuwen, J.F.N., van der Knaap, W.O., Ilyashuk, E., Oberli, F., Ammann, B., 2009. Lateglacial environmental and climatic changes at the Maloja Pass, Central Swiss Alps, as recorded by chironomids and pollen. Quat. Sci. Rev. 28, 1340–1353. https://doi.org/10.1016/j.quascirev.2009.01.007.
Ilyashuk, E.A., Koinig, K.A., Heiri, O., Ilyashuk, B.P., Psenner, R., 2011. Holocene temperature variations at a high-altitude site in the Eastern Alps: a chironomid record from Schwarzsee ob Sölden, Austria. Quat. Sci. Rev. 30, 176–191. https://doi.org/10.1016/j.quascirev.2010.10.008.
Ilyashuk, E.A., Heiri, O., Ilyashuk, B.P., Koinig, K.A., Psenner, R., 2019. The Little Ice Age signature in a 700-year high-resolution chironomid record of summer temperatures in the Central Eastern Alps. Clim. Dynam. 52, 6953–6967. https://doi.org/10.1007/s00382-018-4555-y.
Immler, T., von Siegl, J., 1888. Aufnahme Vermunt-Ochsentaler-Schneeglocken-Schattenspitz Gletscher. Verlag des Deutschen und Österreichischen Alpenvereins.
IPCC, 2014. Climate Change 2014: Synthesis Report. Contribution of Working Groups I, II and III to the Fifth Assessment Report of the Intergovernmental Panel on Climate Change. In: IPCC AR5 Synthesis Report. IPCC, Geneva, Switzerland, p. 151. Geneva, Switzerland.
Ivy-Ochs, S., 2015. Glacier variations in the European Alps at the end of the last glaciation. Cuadernos Invest. Geogr. 41, 295–315. https://doi.org/10.18172/cig.2750.
Ivy-Ochs, S., Kober, F., 2008. Surface exposure dating with cosmogenic nuclides. E&G – Quat. Sci. J. 57, 179–209. https://doi.org/10.3285/eg.57.1-2.7.
Ivy-Ochs, S., Kerschner, H., Reuther, A., Maisch, M., Sailer, R., Schaefer, J., Kubik, P.W., Synal, H.-A., Schlüchter, C., 2006. The timing of glacier advances in the northern European Alps based on surface exposure dating with cosmogenic 10Be, 26Al, 36Cl, and 21Ne. In: Alonso-Zarza, A.M., Tanner, L.H. (Eds.), In Situ-Produced Cosmogenic Nuclides and Quantification of Geological Processes. Geological Society of America.
Ivy-Ochs, S., Kerschner, H., Schlüchter, C., 2007. Cosmogenic nuclides and the dating of Lateglacial and Early Holocene glacier variations: The Alpine perspective. Quat. Int. 164–165, 53–63. https://doi.org/10.1016/j.quaint.2006.12.008.
Ivy-Ochs, S., Kerschner, H., Maisch, M., Christl, M., Kubik, P.W., Schlüchter, C., 2009. Latest pleistocene and Holocene glacier variations in the European Alps. Quat. Sci. Rev. 28 (21–22), 2137–2149. https://doi.org/10.1016/j.quascirev.2009.03.009.
Jennings, A., Andrews, J., Pearce, C., Wilson, L., Olfasdotttir, S., 2015. Detrital carbonate peaks on the Labrador shelf, a 13–7 ka template for freshwater forcing from the Hudson Strait outlet of the Laurentide Ice Sheet into the subpolar gyre. Quat. Sci. Rev. 107, 62–80. https://doi.org/10.1016/j.quascirev.2014.10.022.
Joerin, U.E., Stocker, T.F., Schlüchter, C., 2006. Multicentury glacier fluctuations in the Swiss Alps during the Holocene. Holocene 16 (4), 697–704. https://doi.org/10.1191/0959683606hl946rp.
Joerin, U.E., Nicolussi, K., Fischer, A., Stocker, T.F., Schlüchter, C., 2008. Holocene optimum events inferred from subglacial sediments at Tschierva Glacier, Eastern Swiss Alps. Quat. Sci. Rev. 27, 337–350. https://doi.org/10.1016/j.quascirev.2007.10.016.
Jomelli, V., Chapron, E., Favier, V., Rinterknecht, V., Braucher, R., Tournier, N., Gascoin, S., Marti, R., Galop, D., Binet, S., Deschamps-Berger, C., Tissoux, H., Aumaitre, G., Bourlès, D.L., Keddadouche, K., 2020. Glacier fluctuations during the Late Glacial and Holocene on the Ariège valley, northern slope of the Pyrenees and reconstructed climatic conditions. Mediterranean Geosci. Rev. 2, 37–51. https://doi.org/10.1007/s42990-020-00018-5.
K. u. k. Militärgeographisches Institut, 1908-1915. Spezialkarte 1:75000 - Blatt 5244. K. U. K. Militärgeographisches Institut, Vienna.
K. u. k. Militärgeographisches Institut, 1934-1937. Spezialkarte 1:75000 - Blatt 5244. K. U. K. Militärgeographisches Institut, Vienna.
Kaplan, M.R., Strelin, J.A., Schaefer, J.M., Denton, G.H., Finkel, R.C., Schwartz, R., Putnam, A.E., Vandergoes, M.J., Goehring, B.M., Travis, S.G., 2011. In-situ cosmogenic Be-10 production rate at Lago Argentino, Patagonia: implications for late-glacial climate chronology. Earth Planet Sci. Lett. 309, 21–32. https://doi.org/10.1016/j.epsl.2011.06.018.
Kaser, G., Grosshauser, M., Marzeion, B., 2010. Contribution potential of glaciers to water availability in different climate regimes. PNAS 107, 20223–20227. https://doi.org/10.1073/pnas.1008162107.
Kasper, M., 2013. Silvretta historica – Zeitreise durch die Silvretta. Heimatschutzverein Montafon, Schruns, p. 256.
Kelly, M.A., Kubik, P.W., Von Blanckenburg, F., Schlüchter, C., 2004. Surface exposure dating of the Great Aletsch Glacier Egesen moraine system, western Swiss Alps, using the cosmogenic nuclide Be-10. J. Quat. Sci. 19, 431–441. https://doi.org/10.1002/jqs.854.
Kelly, M.A., Lowell, T.V., Applegate, P.J., Phillips, F.M., Schaefer, J.M., Smith, C.A., Kim, H., Leonard, K.C., Hudson, A.M., 2015. A locally calibrated, late glacial Be-10 production rate from a low-latitude, high-altitude site in the Peruvian Andes. Quat. Geochronol. 26, 70–85. https://doi.org/10.1016/j.quageo.2013.10.007.
Kerschner, H., Ivy-Ochs, S., 2008. Palaeoclimate from glaciers: examples from the eastern Alps during the alpine lateglacial and early Holocene. Global Planet. Change 60, 58–71. https://doi.org/10.1016/j.gloplacha.2006.07.034.
Kerschner, H., Hertl, A., Gross, G., Ivy-Ochs, S., Kubik, P.W., 2006. Surface exposure dating of moraines in the Kromer valley (Silvretta Mountains, Austria) - evidence for glacial response to the 8.2 ka event in the Eastern Alps. Holocene 16, 7–15.
Koinig, K., Nicolussi, K., Moernaut, J., Huang, J.-J.S., Tessadri, R., Ilyashuk, E., Strasser, M., Psenner, R., Ilyashuk, B., 2019. Timing the Little Ice Age Advance and Fluctuations of a Glacier in the Eastern Alps - a Multi-Proxy Lake Sediment Study, Poster, INQUA 2019, Dublin.
Kothieringer, K., Walser, C., Dietre, B., Reitmaier, T., Haas, J.N., Lambers, K., 2015. High impact: early pastoralism and environmental change during the Neolithic and Bronze Age in the Silvretta Alps (Switzerland/Austria) as evidenced by archaeological, palaeoecological and pedological proxies. Z. Geomorphol. 59, 177–198. https://doi.org/10.1127/zfg_suppl/2015/S-59210.
Kronig, O., Ivy-Ochs, S., Hajdas, I., Christl, M., Wirsig, C., Schlüchter, C., 2018. Holocene evolution of the Triftje- and the Oberseegletscher (Swiss Alps) constrained with Be-10 exposure and radiocarbon dating. Swiss J. Geosci. 111, 117–131. https://doi.org/10.1007/s00015-017-0288-x.
Lal, D., 1988. In situ-produced cosmogenic isotopes in terrestrial rocks. Annu. Rev. Earth Planet Sci. 16, 355–388. https://doi.org/10.1146/annurev.ea.16.050188.002035.
Lal, D., 1991. Cosmic-Ray labeling of erosion surfaces – In situ nuclide production-rates and erosion models. Earth Planet Sci. Lett. 104 (2–4), 424–439. https://doi.org/10.1016/0012-821X(91)90220-C.
Landesamt für Vermessung und Geoinformation, 2019. Vorarlberg Atlas4. Land Vorarlberg, Feldkirch.
Larocque, I., Finsinger, W., 2008. Late-glacial chironomid-based temperature reconstructions for Lago Piccolo di Avigliana in the southwestern Alps (Italy). Palaeogeogr. Palaecol. 257, 207–223. https://doi.org/10.1016/j.palaeo.2007.10.021.
Larocque-Tobler, I., Heiri, O., Wehrli, M., 2010. Late Glacial and Holocene temperature changes at Egelsee, Switzerland, reconstructed using subfossil chironomids. J. Paleolimnol. 43, 649–666. https://doi.org/10.1007/s10933-009-9358-z.
Le Roy, M., Nicolussi, K., Deline, P., Astrade, L., Edouard, J.L., Miramont, C., Arnaud, F., 2015. Calendar-dated glacier variations in the western European Alps during the neoglacial: the mer de Glace record, Mont Blanc massif. Quat. Sci. Rev. 108, 1–22. https://doi.org/10.1016/j.quascirev.2014.10.033.
Le Roy, M., Deline, P., Carcaillet, J., Schimmelpfennig, I., Ermini, M., ASTER Team, 2017. Be-10 exposure dating of the timing of Neoglacial glacier advances in the Ecrins-Pelvoux massif, southern French Alps. Quat. Sci. Rev. 178, 118–138. https://doi.org/10.1016/j.quascirev.2017.10.010.
Luetscher, M., Hoffmann, D.L., Frisia, S., Spötl, C., 2011. Holocene glacier history from alpine speleothems, Milchbach cave, Switzerland. Earth Planet Sci. Lett. 302, 95–106. https://doi.org/10.1016/j.epsl.2010.11.042.
Luterbacher, J., Werner, J.P., Smerdon, J.E., Fernandez-Donado, L., González-Rouco, F.J., Barriopedro, D., Ljungqvist, F.C., Büntgen, U., Zorita, E., Wagner, S., Esper, J., McCarroll, D., Toreti, A., Frank, D., Jungclaus, J.H., Barriendos, M., Bertolin, C., Bothe, O., Brázdil, R., Camuffo, D., Dobrovolný, P., Gagen, M., García-Bustamante, E., Ge, Q., Gómez-Navarro, J.J., Guiot, J., Hao, Z., Hegerl, G.C., Holmgren, K., Klimenko, V.V., Martín-Chivelet, J., Pfister, C., Roberts, N., Schindler, A., Schurer, A., Solomina, O., von Gunten, L., Wahl, E., Wanner, H., Wetter, O., Xoplaki, E., Yuan, N., Zanchettin, D., Zhang, H., Zerefos, C., 2016. European summer temperatures since Roman times. Environ. Res. Lett. 11, 1–12. https://doi.org/10.1088/1748-9326/11/2/024001.
Lüthi, M.P., 2014. Little Ice Age climate reconstruction from ensemble reanalysis of Alpine glacier fluctuations. Cryosphere 8, 639–650. https://doi.org/10.5194/tc-8-639-2014.
Magny, M., 2004. Holocene climate variability as reflected by mid-European lake-level fluctuations and its probable impact on prehistoric human settlements. Quat. Int. 113, 65–79. https://doi.org/10.1016/S1040-6182(03)00080-6.
Magny, M., Leuzinger, U., Bortenschlager, S., Haas, J.N., 2006. Tripartite climate reversal in Central Europe 5600-5300 years ago. Quat. Res. 65, 3–19. https://doi.org/10.1016/j.yqres.2005.06.009.
Magny, M., Galop, D., Bellintani, P., Desmet, M., Didier, J., Haas, J.N., Martinelli, N., Pedrotti, A., Scandolari, R., Stock, A., Vannière, B., 2009. Late-Holocene climatic variability south of the Alps as recorded by lake-level fluctuations at Lake Ledro, Trentino, Italy. Holocene 19, 575–589. https://doi.org/10.1177/0959683609104032.
Mann, M.E., 2002. Little Ice Age. Encyclopedia of Global Environmental Change 1, 504–509.
Mann, M.E., Zhang, Z.H., Hughes, M.K., Bradley, R.S., Miller, S.K., Rutherford, S., Ni, F.B., 2008. Proxy-based reconstructions of hemispheric and global surface temperature variations over the past two millennia. Proc. Natl. Acad. Sci. USA

105, 13252–13257. https://doi.org/10.1073/pnas.0805721105.
Marcott, S.A., Shakun, J.D., Clark, P.U., Mix, A.C., 2013. A reconstruction of regional and global temperature for the past 11,300 years. Science 339, 1198–1201. https://doi.org/10.1126/science.1228026.
Martin, L.C.P., Blard, P.H., Lave, J., Braucher, R., Lupker, M., Condom, T., Charreau, J., Mariotti, V., Davy, E., ASTER Team, 2015. In situ cosmogenic Be-10 production rate in the High Tropical Andes. Quat. Geochronol. 30, 54–68. https://doi.org/10.1016/j.quageo.2015.06.012.
Marzeion, B., Cogley, J.G., Richter, K., Parkes, D., 2014. Attribution of global glacier mass loss to anthropogenic and natural causes. Science 345, 919–921. https://doi.org/10.1126/science.1254702.
Matthews, J.A., Briffa, K.R., 2005. The 'Little Ice Age': Re-evaluation of an evolving concept. Geogr. Ann. 87a, 17–36.
Mayewski, P.A., Rohling, E.E., Stager, J.C., Karlen, W., Maasch, K.A., Meeker, L.D., Meyerson, E.A., Gasse, F., van Kreveld, S., Holmgren, K., Lee-Thorp, J., Rosqvist, G., Rack, F., Staubwasser, M., Schneider, R.R., Steig, E.J., 2004. Holocene climate variability. Quat. Res. 62, 243–255. https://doi.org/10.1016/j.yqres.2004.07.001.
K. u. k. Militärgeographisches Institut, 1887. Dritte Reambulierte Landesaufnahme (Franzisco-Josephinische Landesaufnahme) - Blatt 5244. K. U. K. Militärgeographisches Institut, Vienna.
Moran, A.P., Ivy-Ochs, S., Vockenhuber, C., Kerschner, H., 2017a. First 36Cl exposure ages from a moraine in the northern Calcareous Alps. E&G Quat. Sci. J. 65, 145–155. https://doi.org/10.3285/eg.65.2.03.
Moran, A.P., Kerschner, H., Ivy-Ochs, S., 2016b. Redating the moraines in the Kromer valley (Silvretta mountains) - new evidence for an early Holocene glacier advance. Holocene 26, 655–664.
Moran, A.P., Ivy Ochs, S., Christl, M., Kerschner, H., 2017b. Exposure dating of a pronounced glacier advance at the onset of the late-Holocene in the central Tyrolean Alps. Holocene 27, 1350–1358. https://doi.org/10.1177/0959683617690589.
Moran, A.P., Ivy-Ochs, S., Schuh, M., Christl, M., Kerschner, H., 2016a. Evidence of central Alpine glacier advances during the Younger Dryas-early Holocene transition period. Boreas 45, 398–410. https://doi.org/10.1111/bor.12170.
Nesje, A., Dahl, S.O., Bakke, J., 2004. Were abrupt Lateglacial and early-Holocene climatic changes in northwest Europe linked to freshwater outbursts to the North Atlantic and Arctic Oceans? Holocene 14, 299–310. https://doi.org/10.1191/0959683604hl708fa.
Nicolussi, K., 2010. Jahrringdaten zur nacheiszeitlichen Waldverbreitung in der Silvretta. In: Reitmaier, T. (Ed.), Letzte Jäger, erste Hirten – Hochalpine Archäologie in der Silvretta. Abt. Ur- und Frühgeschichte der Universität Zürich, Zürich, pp. 67–76.
Nicolussi, K., 2011. Gletschergeschichte der Pasterze – Spurensuche in die nacheiszeitliche Vergangenheit. In: Die Pasterze - Der Gletscher am Großglockner. Pustet, Salzburg, pp. 24–27.
Nicolussi, K., 2013. Die historischen Vorstöße und Hochstände des Vernagtferners 1600-1850 AD. Zeitschrift für Gletscherkunde und Glaziologie 45/46, 9–23.
Nicolussi, K., Patzelt, G., 2000. Discovery of early-Holocene wood and peat on the forefield of the Pasterze glacier, eastern Alps, Austria. Holocene 10, 191–199. https://doi.org/10.1191/095968300666855842.
Nicolussi, K., Patzelt, G., 2001. Untersuchungen zur holozänen Gletscherentwicklung von Pasterze und Gepatschferner (Ostalpen). Zeitschrift für Gletscherkunde und Glaziologie 36, 1–87.
Nicolussi, K., Schlüchter, C., 2012. The 8.2 ka event-calendar-dated glacier response in the Alps. Geology 40, 819–822. https://doi.org/10.1130/G32406.1.
Nicolussi, K., Kaufmann, M., Patzelt, G., van der Plicht, J., Thurner, A., 2005. Holocene tree-line variability in the Kauner Valley, Central Eastern Alps, indicated by dendrochronological analysis of living trees and subfossil logs. Veg. Hist. Archaeobotany 14, 221–234. https://doi.org/10.1007/s00334-005-0013-y.
Nicolussi, K., Joerin, U.E., Kaiser, K.F., Patzelt, G., Thurner, A., 2006. Precisely dated glacier fluctuations in the Alps over the last four millennia. In: Price, M.F. (Ed.), Global Change in Mountain Regions. Sapiens Publishing, Dumfrieshire, pp. 59–60.
Nicolussi, K., Kaufmann, M., Melvin, T.M., van der Plicht, J., Schiessling, P., Thurner, A., 2009. A 9111 year long conifer tree-ring chronology for the European Alps: a base for environmental and climatic investigations. Holocene 19, 909–920. https://doi.org/10.1177/0959683609336565.
Nicolussi, K., Dusch, M., Drescher-Schneider, R., Kellerer-Pirklbauer, A., Le Roy, M., Maussion, F., Schlüchter, C., 2019. Glacier evolution in the Alps during the early and mid-Holocene - new results from Tschierva and Pasterze glaciers. In: Poster, International Mountain Conference 2019, Innsbruck.
Nowotny, A., Pestal, M., Rockenschaub, M., 1993. Der geologische Bau der nördlichen Silvrettamasse und die Problematik der geologischen Stellung der Zone von Puschlin. Arbeitstagung Geol. B.-A. 55–91.
Nussbaumer, S.U., Zumbühl, H.J., 2012. The Little Ice Age history of the Glacier des Bossons (Mont Blanc massif, France): a new high-resolution glacier length curve based on historical documents. Clima, Chang. 111, 301–334. https://doi.org/10.1007/s10584-011-0130-9.
Oerlemans, J., 2005. Extracting a climate signal from 169 glacier records. Science 308, 675–677.
Osborn, T.J., Briffa, K.R., 2006. The spatial extent of 20th-century warmth in the context of the past 1200 years. Science 311, 841–844. https://doi.org/10.1126/science.1120514.
Österreichischer Alpenverein, 2019. Gletscherbericht 2017/2018 – Sammelbericht über die Gletschermessungen des Österreichischen Alpenvereins im Jahre 2018. Bergauf 19, 20–29.
PAGES 2k Consortium, 2013. Continental-scale temperature variability during the past two millennia. Nat. Geosci. 6, 339–346. https://doi.org/10.1038/Ngeo1797.
Patzelt, G., 1973. Die neuzeitlichen Gletscherschwankungen in der Venedigergruppe (Hohe Tauern, Ostalpen). Z. Gletscherkd. Glazialgeol. 9, 5–57.
Patzelt, G., 2015. Holozäne Gletscher- und Waldgrenzentwicklung im Bereich des Schlatenkeeses, Venedigergruppe, Osttirol (Österreich). Z. Gletscherkd. Glazialgeol. 47/48, 91–99.
Patzelt, G., 2016. Das Bunte Moor in der Oberfernau (Stubaier Alpen, Tirol) – Eine neu bearbeitete Schlüsselstelle für die Kenntnis der nacheiszeitlichen Gletscherschwankungen der Ostalpen. Jahrbuch der Geologischen Bundesanstalt Band 156, 97–107.
Patzelt, G., Bortenschlager, S., 1973. Die postglazialen Gletscher-und Klimaschwankungen in der Venedigergruppe (Hohe Tauern, Ostalpen). Zeitschrift für Geomorphologie NF, Suppl. Bd 16, 25–72.
Phillips, F.M., Argento, D.C., Balco, G., Caffee, M.W., Clem, J., Dunai, T.J., Finkel, R., Goehring, B., Gosse, J.C., Hudson, A.M., Jull, A.J.T., Kelly, M.A., Kurz, M., Lal, D., Lifton, N., Marrero, S.M., Nishiizumi, K., Reedy, R.C., Schaefer, J., Stone, J.O.H., Swanson, T., Zreda, M.G., 2016. The CRONUS-Earth Project: a synthesis. Quat. Geochronol. 31, 119–154. https://doi.org/10.1016/j.quageo.2015.09.006.
Pindur, P., Heuberger, H., 2010. Zur holozänen Gletschergeschichte im Zemmgrund in den Zillertaler Alpen, Tirol/Österreich (Ostalpen). Z. Gletscherkd. Glazialgeol. 42 (2), 21–89.
Protin, M., Schimmelpfennig, I., Mugnier, J.-L., Ravanel, L., Le Roy, M., Deline, P., Favier, V., Buoncristiani, J.-F., Aumaître, G., Bourlès, D.L., Keddadouche, K., 2019. Climatic reconstruction for the Younger Dryas/Early Holocene transition and the Little Ice Age based on paleo-extents of Argentière glacier (French Alps). Quat. Sci. Rev. 221, 105863. https://doi.org/10.1016/j.quascirev.2019.105863.
Putnam, A.E., Schaefer, J.M., Denton, G.H., Barrell, D.J.A., Finkel, R.C., Andersen, B.G., Schwartz, R., Chinn, T.J.H., Doughty, A.M., 2012. Regional climate control of glaciers in New Zealand and Europe during the pre-industrial Holocene. Nat. Geosci. 5, 627–630. https://doi.org/10.1038/NGEO1548.
Putnam, A.E., Bromley, G.R.M., Rademaker, K., Schaefer, J.M., 2019. In situ 10Be production-rate calibration from a 14C-dated late-glacial moraine belt in Rannoch Moor, central Scottish Highlands. Quat. Geochronol. 50, 109–125. https://doi.org/10.1016/j.quageo.2018.11.006.
Rasmussen, S.O., Andersen, K.K., Svensson, A.M., Steffensen, J.P., Vinther, B.M., Clausen, H.B., Siggaard-Andersen, M.L., Johnsen, S.J., Larsen, L.B., Dahl-Jensen, D., Bigler, M., Röthlisberger, R., Fischer, H., Goto-Azuma, K., Hansson, M.E., Ruth, U., 2006. A new Greenland ice core chronology for the last glacial termination. J. Geophys. Res. Atmos. 111 https://doi.org/10.1029/2005jd006079.
Reichert, B.K., Bengtsson, L., Oerlemans, J., 2002. Recent glacier retreat exceeds internal variability. J. Clim. 15, 3069–3081. https://doi.org/10.1175/1520-0442(2002)015<3069:RGREIV>2.0.CO;2.
Reitmaier, T., 2012. Letzte Jäger, erste Hirten: Hochalpine Archäologie in der Silvretta. Südostschweiz-Buchverl., Glarus Chur, p. 294.
Reitmaier, T., Walser, C., 2016. Pölls Schnapsflasche – Oder was die Archäologen in den Alpen suchen. In: Kasper, M. (Ed.), Mythos Piz Buin : Kulturgeschichte eines Berges. Haymon-Verlag, Innsbruck, Wien, pp. 81–100.
Reitner, J.M., Ivy-Ochs, S., Drescher-Schneider, R., Hajdas, I., Linner, M., 2016. Reconsidering the current stratigraphy of the Alpine Lateglacial: implications of the sedimentary and morphological record of the Lienz area (Tyrol/Austria). E&G Quat. Sci. J. 65, 113–144. https://doi.org/10.3285/eg.65.2.02.
Remy, D., 2012. Waldgrenze und Waldgrenzschwankungen in der Silvretta/Zentralalpen - Funde von Pinus cembra oberhalb der potentiellen Waldgrenze im Oberen Fimbertal. Ber. d. Reinh.-Tüxen-Ges. 24, 61–76.
Rood, D.H., Hall, S., Guilderson, T.P., Finkel, R.C., Brown, T.A., 2010. Challenges and opportunities in high-precision Be-10 measurements at CAMS. Nucl. Instrum. Methods B 268, 730–732. https://doi.org/10.1016/j.nimb.2009.10.016.
Röthlisberger, F., 1976. Gletscher- und Klimaschwankungen im Raum Zermatt, Ferpècle und Arolla. Die Alpen 52, 59–152.
Rutzinger, M., Moran, A., Fischer, A., Gross, G., 2013. Klimawandel und Klimageschichte – Die Gletscher der Silvretta unter wandelnden Klimabedingungen. In: Kasper, M. (Ed.), Silvretta Historica - Zeitreise durch die Silvretta. Heimatschutzverein Montafon, Schruns.
Samartin, S., Heiri, O., Vescovi, E., Brooks, S.J., Tinner, W., 2012. Lateglacial and early Holocene summer temperatures in the southern Swiss Alps reconstructed using fossil chironomids. J. Quat. Sci. 27, 279–289. https://doi.org/10.1002/jqs.1542.
Schaefer, J.M., Denton, G.H., Barrell, D.J.A., Ivy-Ochs, S., Kubik, P.W., Andersen, B.G., Phillips, F.M., Lowell, T.V., Schlüchter, C., 2006. Near-synchronous interhemispheric termination of the last glacial maximum in mid-latitudes. Science 312, 1510–1513. https://doi.org/10.1126/science.1122872.
Schaefer, J.M., Denton, G.H., Kaplan, M.R., Putnam, A., Finkel, R.C., Barrell, D.J.A., Andersen, B.G., Schwartz, R., Mackintosh, A., Chinn, T., Schluchter, C., 2009. High-frequency Holocene glacier fluctuations in New Zealand differ from the northern signature. Science 324, 622–625. https://doi.org/10.1126/science.1169312.
Schaefli, B., Manso, P., Fischer, M., Huss, M., Farinotti, D., 2019. The role of glacier retreat for Swiss hydropower production. Renew. Energy 132, 615–627. https://doi.org/10.1016/j.renene.2018.07.104.
Schimmelpfennig, I., Schaefer, J.M., Akcar, N., Ivy-Ochs, S., Finkel, R.C., Schlüchter, C., 2012. Holocene glacier culminations in the Western Alps and their hemispheric relevance. Geology 40, 891–894. https://doi.org/10.1130/G33169.1.
Schimmelpfennig, I., Schaefer, J.M., Akçar, N., Koffman, T., Ivy-Ochs, S., Schwartz, R.,

Finkel, R.C., Zimmerman, S., Schlüchter, C., 2014. A chronology of Holocene and Little Ice Age glacier culminations of the Steingletscher, Central Alps, Switzerland, based on high-sensitivity beryllium-10 moraine dating. Earth Planet Sci. Lett. 393, 220–230. https://doi.org/10.1016/j.epsl.2014.02.046.

Schimmelpfennig, I., Le Roy, M., Deline, P., Schoeneich, P., Carcaillet, J., Bodin, X., ASTER Team, 2019. Holocene Dynamics of Arsine Glacier (Ecrins Massif, French Alps) Inferred from 10Be Dating. Poster, INQUA 2019, Dublin.

Schindelwig, I., Akçar, N., Kubik, P.W., Schlüchter, C., 2012. Lateglacial and early Holocene dynamics of adjacent valley glaciers in the Western Swiss Alps. J. Quat. Sci. 27, 114–124. https://doi.org/10.1002/jqs.1523.

Schmidt, R., Kamenik, C., Tessadri, R., Koinig, K.A., 2006. Climatic changes from 12,000 to 4,000 years ago in the Austrian Central Alps tracked by sedimentological and biological proxies of a lake sediment core. J. Paleolimnol. 35, 491–505. https://doi.org/10.1007/s10933-005-2351-2.

Schneebeli, W., 1976. Untersuchungen von Gletscherschwankungen im Val de Bagnes. Die Alpen 52, 5–57.

Schuster, R., 2015. Zur Geologie der Ostalpen. Abh. Geol. B.-A. 64, 143–165.

Simonneau, A., Chapron, E., Garçon, M., Winiarski, T., Graz, Y., Chauvel, C., Debret, M., Motelica-Heino, M., Desmet, M., Di Giovanni, C., 2014. Tracking Holocene glacial and high-altitude alpine environments fluctuations from minerogenic and organic markers in proglacial lake sediments (Lake Blanc Huez, Western French Alps). Quat. Sci. Rev. 89, 27–43. https://doi.org/10.1016/j.quascirev.2014.02.008.

Solomina, O.N., Bradley, R.S., Hodgson, D.A., Ivy-Ochs, S., Jomelli, V., Mackintosh, A.N., Nesje, A., Owen, L.A., Wanner, H., Wiles, G.C., Young, N.E., 2015. Holocene glacier fluctuations. Quat. Sci. Rev. 111, 9–34. https://doi.org/10.1016/j.quascirev.2014.11.018.

Solomina, O.N., Bradley, R.S., Jomelli, V., Geirsdottir, A., Kaufman, D.S., Koch, J., Mckay, N.P., Masiokas, M., Miller, G., Nesje, A., Nicolussi, K., Owen, L.A., Putnam, A.E., Wanner, H., Wiles, G., Yang, B., 2016. Glacier fluctuations during the past 2000 years. Quat. Sci. Rev. 149, 61–90. https://doi.org/10.1016/j.quascirev.2016.04.008.

Spindler, K., 1994. The Man in the Ice: The discovery of a 5,000-year-old body reveals the secrets of the Stone Age. Harmony Books, New York, p. 305.

Stone, J.O., 2000. Air pressure and cosmogenic isotope production. J. Geophys. Res. Sol. Ea 105, 23753–23759. https://doi.org/10.1029/2000jb900181.

Strelin, J.A., Kaplan, M.R., Vandergoes, M.J., Denton, G.H., Schaefer, J.M., 2014. Holocene glacier history of the Lago Argentino basin, southern Patagonian icefield. Quat. Sci. Rev. 101, 124–145. https://doi.org/10.1016/j.quascirev.2014.06.026.

Thornalley, D.J., Elderfield, H., McCave, I.N., 2009. Holocene oscillations in temperature and salinity of the surface subpolar North Atlantic. Nature 457, 711–714. https://doi.org/10.1038/nature07717.

Tinner, W., Kaltenrieder, P., 2005. Rapid responses of high-mountain vegetation to early Holocene environmental changes in the Swiss Alps. J. Ecol. 93, 936–947. https://doi.org/10.1111/j.1365-2745.2005.01023.x.

Vaughan, D.G., Comiso, J.C., Allison, I., Carrasco, J., Kaser, G., Kwok, R., Mote, P., Murray, T., Paul, F., Ren, J., Rignot, E., Solomina, O., Steffen, K., Zhang, T., 2013. Observations: Cryosphere. In: Stocker, T.F., Qin, D., Plattner, G.-K., Tignor, M., Allen, S.K., Boschung, J., Nauels, A., Xia, Y., Bex, V., Midgley, P.M. (Eds.), Climate Change 2013: The Physical Science Basis. Contribution of Working Group I to the Fifth Assessment Report of the Intergovernmental Panel on Climate Change. Cambridge University Press, Cambridge, UK and New York, USA.

Vorarlberger Illwerke, A.G., 2017. Integrierter Geschäfts- und Nachhaltigkeitsbericht, p. 113. Bregenz.

Vorndran, G., 1968. Untersuchungen zur Aktivität der Gletscher: dargestellt an Beispielen aus der Silvrettagruppe, Kiel, pp. 129 S., Ill., graph. Darst. u. Kt.

Wanner, H., Beer, J., Butikofer, J., Crowley, T.J., Cubasch, U., Fluckiger, J., Goosse, H., Grosjean, M., Joos, F., Kaplan, J.O., Kuttel, M., Muller, S.A., Prentice, I.C., Solomina, O., Stocker, T.F., Tarasov, P., Wagner, M., Widmann, M., 2008. Mid- to Late Holocene climate change: an overview. Quat. Sci. Rev. 27, 1791–1828. https://doi.org/10.1016/j.quascirev.2008.06.013.

Wanner, H., Solomina, O., Grosjean, M., Ritz, S.P., Jetel, M., 2011. Structure and origin of Holocene cold events. Quat. Sci. Rev. 30, 3109–3123. https://doi.org/10.1016/j.quascirev.2011.07.010.

WGMS, 2018. Fluctuations of Glaciers Database. World Glacier Monitoring Service, Zürich.

Wipf, A., 2001. Gletschergeschichtliche Untersuchungen im spät- und postglazialen Bereich des Hinteren Lauterbrunnentals (Berner Oberland, Schweiz). Geograph. Helv. 56, 133–144. https://doi.org/10.5194/gh-56-133-2001.

Wirsig, C., Ivy-Ochs, S., Akçar, N., Lupker, M., Hippe, K., Wacker, L., Vockenhuber, C., Schlüchter, C., 2016. Combined cosmogenic Be-10, in situ C-14 and Cl-36 concentrations constrain Holocene history and erosion depth of Grueben glacier (CH). Swiss J. Geosci. 109, 379–388. https://doi.org/10.1007/s00015-016-0227-2.

Young, N.E., Schaefer, J.M., Briner, J.P., Goehring, B.M., 2013. A Be-10 production-rate calibration for the Arctic. J. Quat. Sci. 28, 515–526. https://doi.org/10.1002/jqs.2642.

Young, N.E., Briner, J.P., Miller, G.H., Lesnek, A.J., Crump, S.E., Thomas, E.K., Pendleton, S.L., Cuzzone, J., Lamp, J., Zimmerman, S., Caffee, M., Schaefer, J.M., 2020. Deglaciation of the Greenland and Laurentide ice sheets interrupted by glacier advance during abrupt coolings. Quat. Sci. Rev. 229 https://doi.org/10.1016/j.quascirev.2019.106091.

Zumbühl, H.J., Nussbaumer, S.U., 2018. Little Ice Age Glacier history of the Central and Western Alps from pictorial documents. Geogr. Res. Lett. 44 (1), 115–136. https://doi.org/10.18172/cig.3363.